SYNTHESIS, STRUCTURE AND CHARACTERIZATION OF SILVER DOPED DIAMOND LIKE CARBON THIN FILMS

by

PANKAJ JYOTI HAZARIKA

Presented to the Faculty of the Graduate School of

The University of Texas at Arlington in Partial Fulfillment

of the Requirements

for the Degree of

MASTER OF SCIENCE IN MATERIAL SCIENCE AND ENGINEERING

THE UNIVERSITY OF TEXAS AT ARLINGTON

December 2007

ACKNOWLEDGEMENTS

The author would like to express his sincere gratitude to Dr.Efstathios I. Meletis, his research advisor, for his excellent guidance and constant encouragement throughout his research work. He would like to thank Dr. Yaowu Hao and Dr. Micheal Jin for their participation as his committee members.

He also wants to thank Dr. Shaoxin You for his help during the research work. He wants to thank Dr. Yuhang Cheng for his help during the system designing. He would also like to thank Pruthul Desai for his enduring help during the equipment assembling and also in the research work. Further, the author would like to mention the various UTA labs that helped in his research, Surface and Nano Engineering lab (SaNEL), Characterization Center for Materials and Biology, Nanotechnology Research and Teaching Facility and Automation & Robotics Research Institute (ARRI).

The author wishes to thank his friends Sunil Singh Gusain, Parthen Parik, Siddarth Pandya and Siddarth Bojudu for their moral support and help. The author also wishes to express his sincere appreciation to his parents, brother, sister, brother-in-law and sister-in-law and his niece and nephews for their constant support and encouragement.

November 26, 2007

ABSTRACT

SYNTHESIS, STRUCTURE AND CHARCTERIZATION OF SILVER DOPED DIAMOND LIKE CARBON THIN FILMS

Publication No. _____

Pankaj Jyoti Hazarika, M.S.

The University of Texas at Arlington, 2007

Supervising Professor: Dr.Efsthathios I. Meletis

Diamond like carbon (DLC) films have gained grounds in the biomedical field as an inert, biocompatible, low friction and wear resistant coating and are widely used in heart valves, coronary artery stents, dental implants, knee prosthesis and other vascular devices. In addition, Ag nanoparticles/films can prevent the formation of biofilm on biomedical implants by degrading the metabolic activities like permeability and respiration and also impair DNA replicability. Thus, Ag-doped DLC (Ag-DLC) can serve as a multifunctional bio coating combining desirable antibacterial and physical/ mechanical characteristics. In the present study, Ag-DLC films were synthesized utilizing a hybrid Plasma CVD and Magnetron sputtering process in a

CH_4/Ar glow discharge. Nanocomposite films containing Ag nanoparticles in an amorphous DLC matrix with various amounts of Ag were synthesized and characterized by Transmission Electron Microscope (TEM), Fourier Transform Infrared Spectroscopy (FTIR) and X-ray Photoelectron Spectroscopy (XPS). Tribological experiments were performed to assess the frictional behavior and wear resistance of the Ag-DLC films as a function of Ag content. Anodic polarization experiments were conducted to characterize the electrochemical behavior of the Ag-DLC films. TEM results revealed that Ag nanoparticles of 4-7 nm in size were uniformly distributed in an amorphous DLC matrix. Microhardness of DLC films exhibited a hardness of 22 GPa and it gradually decreased with increasing Ag content in the films. Wear rate of DLC film was 1.9×10^{-8} mm^3/Nm and it increased to 8×10^{-7} mm^3/Nm for Ag-DLC (5% Ag) film. Electrochemical behavior experiments showed that Ag-DLC films exhibited an inert behavior compared to the pure silver.

TABLE OF CONTENTS

LIST OF ILLUSTRATIONS

LIST OF TABLES

CHAPTER 1

INTRODUCTION

1.1 Diamond-like carbon thin films

Nanotechnology has marked the dawn of a new era in respect to unique material properties and has enthralled the world by its wide gamut of applications in electronics, biotechnology and various mechanical properties. Carbon has drawn the attention of researchers because of its ability to exist in various forms like sp^3 hybridized diamond and sp^2 hybridized graphitic structure. Diamond has high hardness, wide band gap, chemical resistance, wide band gap, low wear whereas graphite is soft, high wear rate and good electrical conductivity [1].

Diamond-like carbon (DLC), a metastable form of amorphous carbon, has drawn the attention due to its low friction coefficient and wear rate, chemical inertness and high hardness. It is widely used in automobiles, industrial wear parts like dies and molds, magnetic storage devices and also as a biomedical coating. The drawbacks of DLC are that it starts graphitization above 350°C and has low toughness and adhesion to the substrate. These issues can be rectified to a large extent by doping DLC films with metals like Cr, Si, Ti, W and Ag. Another advantage of doping is that the doping elements attribute additional desirable properties to the films like corrosion stability in case Cr-DLC and antibacterial properties in Ag-DLC [1,2,3,4,].

1.2 Silver- a good antibacterial agent

Nosocomial infection in implants is a major concern in the medical world and demands effective means to tackle the challenges. It has been estimated by the Centers for disease control that nosocomial infections incurred a cost more than $2300 per patient for diagnosis and treatment. In addition to that the infection cost to hospitals is around $4.8 billion annually in extended care and treatment [5, 6]. Biomedical implants serve as a major source of hospital related bacterial infection when implanted inside the body. This has been a major challenge over the years and has triggered lots of research related to the development of antibacterial surface coatings.

Researchers are always focused on developing various techniques which should be effective against the infections associated with the surgical implants. Silver, being one of the toxic elements, has attracted their attention. Over the years, silver particles have proved to be effective against a range of bacteria and also against other pathogens.

Silver has been a potential antibacterial agent from the days of yore. Silver is effective against a wide range of spectrum including gram negative enterobacteria (e.g. Pseudomonas aeruginosa), yeast (e.g.Candida albicans) and gram positive cocci (esp. mutliresistant coagulase-positive and –negative staphylococci and enterococci [6]. Silver salts have long been used in wounds and now with the emergence of nanotechnology, research is focused on the use of silver nanoparticles as an effective antibacterial agent. It has been experimentally seen that silver nanoparticles (esp. in the size range of 1-10 nm) attach to the surface of gram negative bacteria, degrade its

metabolic activities like permeability and respiration and also impair DNA replicability [2,7].

1.3 Efficacy of Ag-DLC in biomedical world

DLC has gained grounds in biomedical world as a inert, biocompatible, low friction and wear resistant coating and it is widely used in heart valves, coronary artery stents, dental implants, knee prosthesis and other vascular devices [1, 2, 3, 4]. Addition of metals to DLC reduces stresses in the film and also adds up the beneficial effect of an alloying element [5]. So, a combination of silver and DLC would result in a good and effective antibacterial coating for implants. Ag^{+} would be released into the blood by electrochemical reaction and would protect the implant from biofilm formation.

CHAPTER 2

OBJECTIVE

The goal of the present study was to develop Ag-doped DLC films using combined magnetron sputtering and plasma chemical vapor deposition (CVD) system which will be effective in prevention of bio film formation on the prosthesis implant so that it serves as an antibacterial coating as well as improve the tribological properties of the implants for the effective function of the implants.

The objective was to incorporate silver nanoparticles in the network of DLC which will have high chemical activity due to high surface to volume ratio and study their behavior in PBS solution.

The main objectives of this research are:

1. Study the effect of processing parameters on the characteristics of Ag-DLC films using hybrid magnetron sputtering and plasma CVD.
2. Study the structure of Ag nanoparticles in the DLC matrix.
3. Study the tribological behavior of DLC and Ag-DLC films.
4. Study the electrochemical behavior of Ag-DLC films.
5. Study the effect of Ag doping on electrical resistance in DLC.

CHAPTER 3

LITERATURE REVIEW

3.1 DLC thin films

After the discovery of DLC in 1970 by Aisenberg and Chabot, it has drawn the attention of technologists all over the world due to its high wear resistance, low friction, high hardness, chemical inertness and biocompatibility. Carbon exists in three hybridization states: - sp^1, sp^2 and sp^3. Diamond is characterized by sp^3 hybridization, where each carbon is bonded tetrahedrally to other carbon atom by strong σ bond resulting in a hard structure. On the other hand, graphite has trigonally sp^2 hybridized in which σ bond is along the plane and π bond is normal to the plane. Graphite has strong interlayer σ bond but weak Van der Waals forces between the layers. As a result, the different sheets of graphite slide over one another, making graphite a soft material [1, 9, 10].

Since DLC has both sp^2 and sp^3, its properties lie midway between diamond and graphite. The sp^2 / sp^3 depend on the deposition parameters, presence of other elements and on the hydrogen content [1, 9, 10, 11, 12]. DLC can be categorized to various forms depending on sp^3, sp^2 and hydrogen as shown on the ternary phase diagram in Figure 3.1.

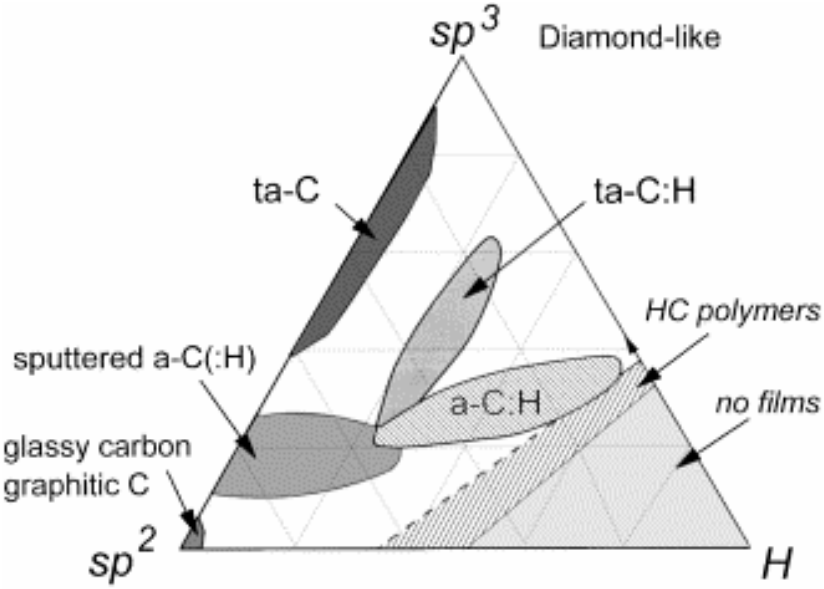

Figure 3.1 Ternary phase diagram of carbon-hydrogen alloys.

Table 3.1 Properties of different carbon forms [1].

	sp3 %	**Hardness GPa**	**H %**	**Density g/cm^3**	**Gap (eV)**
Diamond	100	100	--	3.5	55
Graphite	0	-	--	2.267	0
a-C (evaporated)	0	3	--	1.9	0.4-0.7
a-C (Sputtered)	5	3	--	2.2	0.5
Ta-C	80-88	80	--	3.1	2.5
a-C-H (hard)	40	10-20	30-40	1.6-2.2	1.1-1.7
a-C-H (soft)	60	< 10	40-50	1.2-1.6	1.7-4

3.1.1 DLC synthesis techniques

The most common way to synthesize DLC is either plasma CVD or thermal CVD. In thermal CVD, the substrate is exposed to around 800° - 900°C in carbonaceous precursor gas environment. DLC is formed on the substrate due to chemical decomposition of the precursor molecule. The other way of DLC deposition is plasma CVD where plasma is used to deposit Carbon from a solid state carbon target or from a carbon precursor gas environment. In magnetron sputtering, graphite is sputtered by Ar ions and deposited on the substrate. Another method is ion beam deposition where carbon ions are produced by the plasma sputtering of a graphite cathode in an ion source. Carbon ions are then accelerated to form an ion beam and finally deposit as DLC [1].

The method of DLC deposition from gas precursors has gained grounds over the years. In this method, hydrocarbon gases like CH_4, C_2H_2, C_2H_6, etc. are allowed to flow into the vacuum chamber with optimized Ar dilution ratio. This method is very popular for depositing a-C-H films. The major advantages are low deposition temperature, high deposition rate, good quality films and low contamination [1, 13, 14, 15].

In dc biased plasma CVD, normally the chamber acts as the anode and the substrate is the cathode. The chamber is normally grounded and a negative bias voltage is applied on the substrate plate as shown in Figure 3.2.

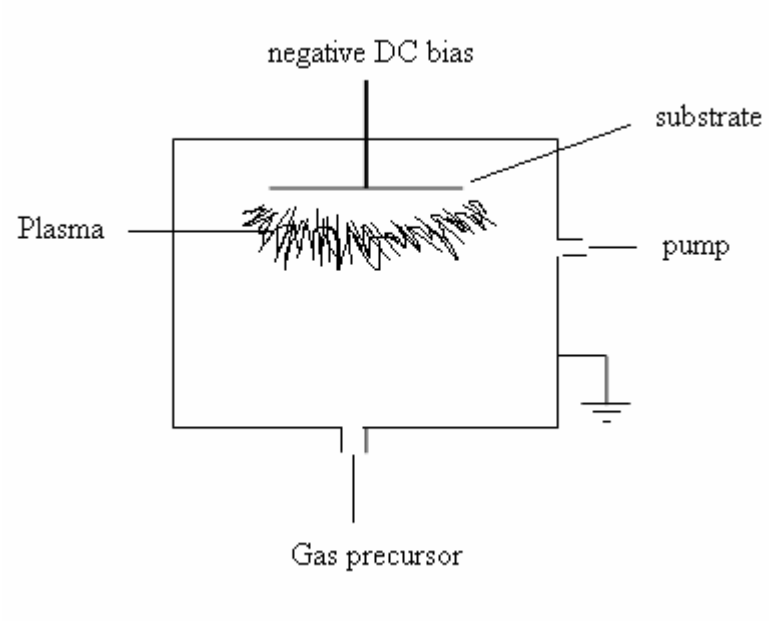

Figure 3.2 DLC deposition by dc biased plasma CVD.

Plasma is created by applying a substrate bias voltage ranging from -100 V to -1000 V and the chamber pressure is maintained from 10 mtorr to 100 mtorr. The bias voltage ionizes the gas precursor molecule and it finally gets deposited on the substrate. The applied voltage and gas pressure decides the impinging energy of the ions and thus regulates the sp^3 /sp^2 ratio in the a-C: H film. The key parameters for getting good smooth films are the bias voltage, working pressure and the hydrogen content in the precursor. The bias voltage and pressure decide the sp^3 /sp^2 ratio and deposition rate of the film whereas hydrogen in DLC plays a very important role in lowering surface energy by passivating the dangling bonds and as such lowers the friction. In addition to this, it helps in stabilizing the sp^3 bonds. The hydrogen content depends on the energy of the incident ions, the ratio of the gases and the type of

precursor gas. If the number of hydrogen atoms in the gas molecule increases, then the friction coefficient decreases due more surface passivation [1, 13, 14, 15, 16].

3.1.2 Metal doped DLC films

Typically, DLC films have high internal stresses which limit the thickness of the films. This problem is addressed by adding metal atoms to the DLC network in order to improve the mechanical properties by relaxing internal stress and also it adds new phase to the films with the potential to provide new functionality. Metal –DLC (Me-DLC) films are commonly synthesized by reactive sputtering of a metal target in argon and hydrocarbon environment or by sputtering both metal and graphite targets. Corbella et al. [13] synthesized Me-DLC containing metals like W, Mo, Nb, Ti using rf PECVD and pulsed dc magnetron sputtering of the targets in argon and methane gas mixture. It was observed that the deposition rate is affected by methane dilution as shown in Figure 3.3.

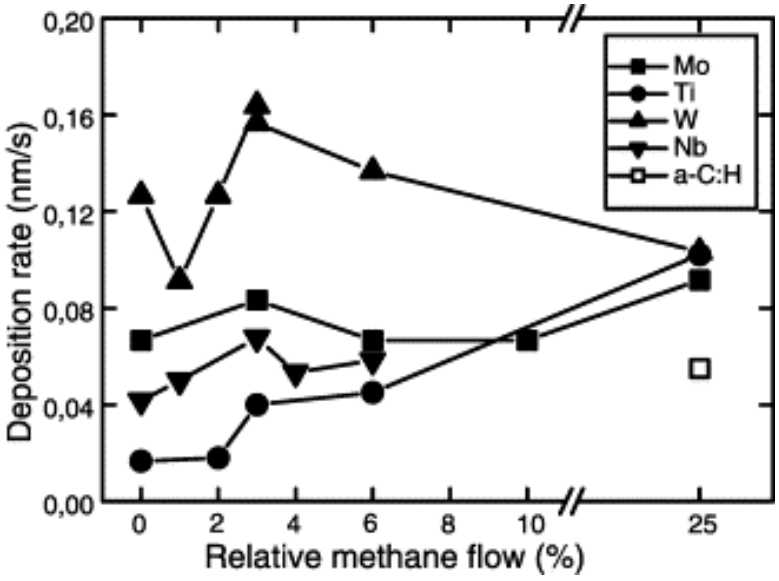

Figure 3.3 Deposition rate vs relative methane flow of Me-DLC films [13].

Kalges and Memming [17] reported that low friction was observed for Me-DLC provided that the carbide forming metal is present at low level. In both DLC and Me-DLC, the low friction is attributed to the transfer layer formation [18]. Experimental evidences have shown that doping Me into the DLC matrix modifies the tribological properties. The wear rate increases but there was not much difference in the friction coefficient compared to DLC.

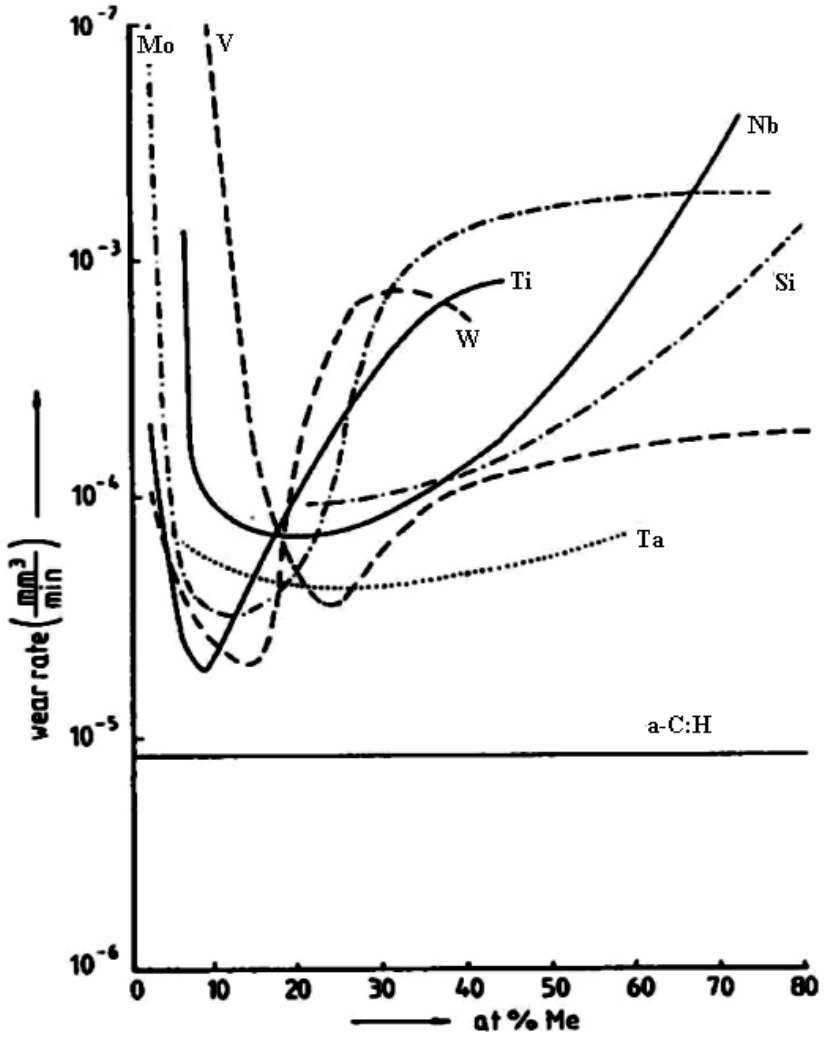

Figure 3.4 Abrasive wear rate of Me-DLC as a function of at% metal [17], 'Calo Test' apparatus was used with aqueous suspensions of 5 μm Al_2O_3 particles.

Me-DLC films have gained grounds for the ability to modify the properties of DLC films by adding the alloying properties. Ali et al. [3] studied the potential application of Cr-DLC film for seeding human micro-vascular endothelial cell on mechanical heart valves. Ag-DLC has shown desirable antibacterial and mechanical properties for biomedical applications [8, 24]. Ag^+ and Ag nanoparticles release into the biological environment and are effective in killing of bacteria. Other Me-DLC like WC-DLC, W-DLC, Ti-DLC, Nb-DLC have shown good mechanical and tribological properties [3, 13, 17, 18].

3.1.3 Wear induced graphitization

Liu and Meletis [19] proposed that during sliding on DLC films, graphitization occurs at the contact area resulting in low friction coefficient. DLC is a metastable amorphous film and it can transform to graphite when the energy barrier for transformation of sp^3 to stable sp^2 graphite is overcome. It has been reported that sp^3 C-C domains transform to sp^2 graphite at about 400°C [19]. The heat generated during sliding, provides the energy to the sp^3 carbon structure. In addition, it was suggested that shear stresses in the surface layer provide the strain energy for the transformation of DLC to graphite layer after the release of hydrogen [19, 20].

3.2 Biocompatibilty of DLC and Ag-DLC thin films

Hauert [21] in his review paper on the biological application of DLC has suggested that DLC can be used in blood contacting implants such as heart valves and stents and can also be used in load bearing joints. In addition to the excellent biocompatibity, it decreases thrombus formation. Mitura et al. [22] conducted

biotolerance test of DLC by implanting DLC coated stainless steel disk into guinea pigs. After 52 weeks of test, there was neither any phagocytic reaction nor any corrosion of the coating. In addition to that, the internal organs did not show any pathomorphological changes. Thus, DLC proves to be a very desirable coating for biomedical implants [23]. The addition of dopants to DLC network reduces compressive stresses and improves adhesion so that thick films can be deposited. Narayan et al. [8] deposited Ag in DLC using pulsed laser deposition with mutlicomponet target and deposited a functionally gradient composite film. They deposited high metal concentration near the substrate interface and gradually diminishing the metal concentration towards the surface of the film. The high Ag concentration near the substrate interface reduced the compressive stresses and the low Ag near the surface attributed high hardness and Young's modulus. The composite film thus obtained showed good adhesion and good hardness. The addition of silver decreased the hardness to around 30-35 GPa compared to DLC and the film showed good antibacterial activity. Moreover, the Ag nanopaticles self assembled in the DLC matrix. The authors have attributed this arrangement to the high surface energy of silver relative to carbon. Oswald ripening did not occur and silver nanoparticles of uniform sizes were obtained. Lungu [24] studied the effect of variation of Gr/Ag target ratio on the coefficient of friction of DLC-Ag and attributed the decrease of coefficient of friction to the nanoscale grain size effect. With the increase in ratio, a transition from sp^2 C-C to sp^3 bond was observed and the best frictional properties were observed in a optimum ratio sp^2 and sp^3 bonds.

3.2.1 Biofilm formation on implants

Furno et al. [25, 26] have broadly classified the implantable device in three categories: category I devices are those which are totally implanted and are at risk mainly at insertion while category II and III devices, like central venous access devices and urinary catheters, which are incompletely implanted and have periods of risk extending throughout their use. Category I devices such as prosthetic hips, knee joints, prosthetic heart valves, have a short period of risk and require antimicrobial protection soon after they are implanted to prevent infection.

Table 3.2 Incidence of infection in medical implants [26].

Implant	**Site**	**Infection rate**
Category I		
Prosthetic hip / knee joint	Hip/knee	1 – 3 %
Vascular grafts	Thoracic aorta	1 %
Hydrocephalus shunts	Brain to abdomen	3 – 6 %
Prosthetic heart valves	Heart	1.5 %
Category II		
Central venous catheters(cuffed)	Central venous system	3 – 10 %
CAPD catheters	Abdominal wall/peritoneum	1.3 per patient/year
Category III		
Voice prosthesis	Trachea/esophagus	100 %

The main problem associated with the implants is the microbial adhesion to the implant and once adhesion had occurred it leads to the development of biofilm which is invulnerable to most of the therapeutic drugs [25, 26]. As soon as an implant is inserted into the body, a protein layer is formed surrounding the devices and this layer serves as the proliferating site of the microbes and finally develops into a thick layer of bacteria. This layer is unaffected by most of the drugs and also protects itself from antibodies [25, 26, 27]. So, in order to prevent the biomaterial –related infections (BRIs), the adhesion of bacteria onto the implants should be restricted or some toxic material should be used. Furno and Bayston [26] have proposed that in order to prevent BRIs, it is necessary to develop materials with antimicrobial activity that will prevent BRIs in the devices and do not provoke microbial resistance. Silver is an effective antimicrobiant and provide resistance in the formation of biofilm.

3.2.2 Antibacterial behavior of Silver.

Klueh et al. [6] studied the effect of silver coating on poly ethylene terephthalte (PET), which is used in heart valves sewing cuffs, found that silver coating reduced the growth rate of *staphylococcus epidermis(SE) bacteria,* by an order of 5 – 6 times and also reduced the adhesion of bacteria to the fabric by an order of 2. Bacterial adhesion to sewing cuffs of heart valves and subsequent formation of biofilm is a major problem and the use of a antibacterial coating seems to be a probable solution to the problem. Klueh et al. have elucidated the antibacterial action of silver and suggested that Ag^{+} forms insoluble compounds with sulfhydryl groups in the cell wall, which are parts of various enzymes involved in transmembrane energy generation and electrolyte

transport. In addition to that, Ag^+ blocks the respiratory chain of bacteria and it enters the cell and binds with bacterial DNA and causes denaturation by displacing hydrogen bonds between adjacent purines and pyrimidines.

The effect of Ag^+ on the morphological changes of E.Coli was clearly illustrated by Feng et al. [2]. He showed that Ag^+ resulted in formation of a dense condensed DNA and it denatured its replication abilities. Ag^+ also reacted with the thiol group of the protein and finally inactivated its enzymatic activity.

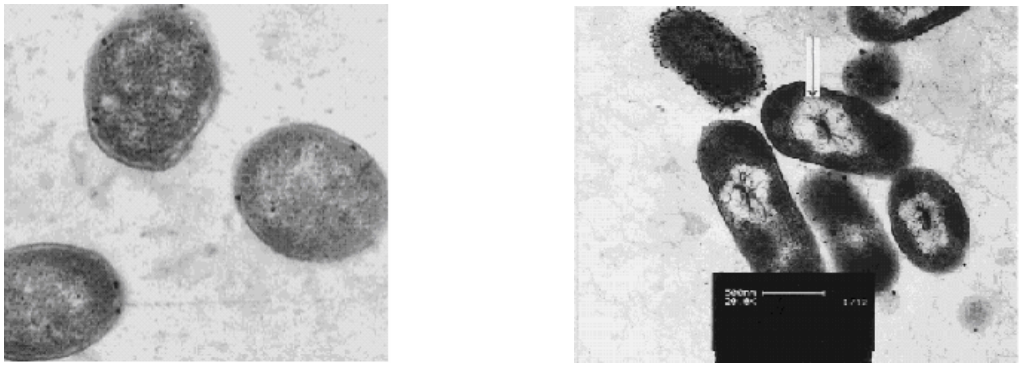

(a) (b)

Figure 3.5 Effect of Ag on E.coli. (a) Internal structure of untreated E.coli (b) Silver ion treated E.coli showing the condensed DNA mass [4].

3.2.3 Silver –DLC and silver coated devices

In the view of the beneficial effects of silver, DLC films incorporated with cytotoxic elements like silver and copper have been synthesized and tested in vitro microbial environments. In aqueous media, Me-DLC forms an electrochemical cell and triggers the release of metallic ions into the media. It is seen that metallic components dissolved in the media, hinders the microbe attachment, growth and proliferation.

Human body can tolerate up to 10 mg/L of silver ion concentration without any side effects [26] and beyond that silver poisoning occurs. Morrison et al. [28] have tested Ag-DLC, Pt-DLC and a conjunction of AgPt-DLC and tested their electrochemical behavior in PBS solution with pH value 7.4 ± 0.01. They obtained a self assembled DLC Ag and DLC Pt composite film and have attributed its formation to the high surface energy of noble metals relative to carbon.

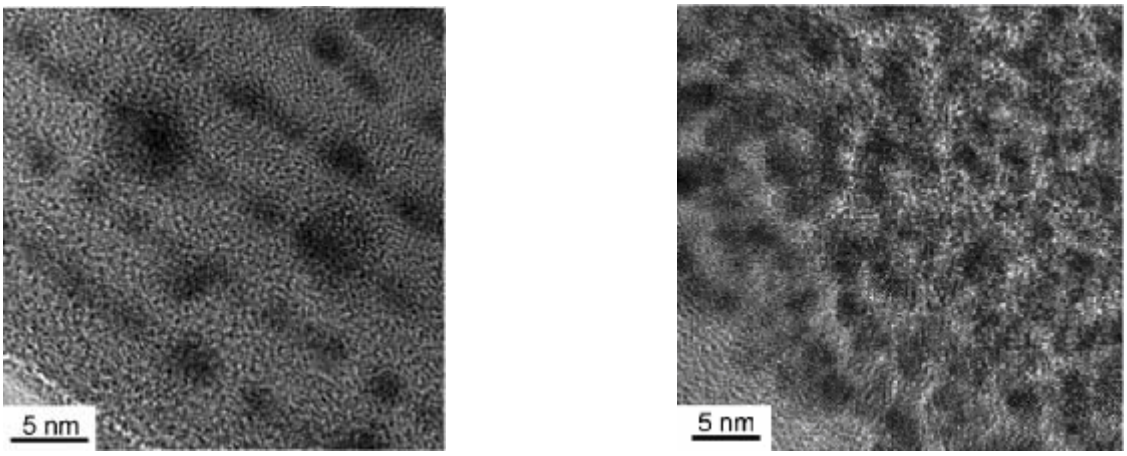

(a) (b)

Figure 3.6 TEM images of Ag-DLC and Ag-Pt DLC films. (a) Bright-field transmission electron micrograph of a DLC-Ag composite film. Silver nanoparticles self-assemble into arrays (dark regions) within the DLC matrix (light regions). (b) Bright-field transmission electron micrograph of a DLC-Pt composite film. Platinum nanoparticles self-assemble into arrays (dark regions) within the DLC (light regions) [28].

Morrison et al. [28] also conducted antibacterial testing and found that Ag–DLC and Ag-Pt DLC provides an incubation period of around 48 and 72 hrs during which the coating had lower bacterial colonization. Ag–DLC showed a 50 % less colonization and Ag-Pt DLC showed a significant value of 90% less colonization than

the uncoated substrate. Deposition of titanium/silver also showed decreased in biofilm formation and enhanced antimicrobial acitivity [29].

Schierholz et al. [30] in their review paper have suggested that silver coated devices are effective when they deliver high concentration of Ag^+ with minimal cytotoxic effects. Dowling et al. [31] have shown that addition of 1 % Pt into Ag coating increases Ag^+ concentration formation, which resulted in enhanced antibacterial activity of the coating with no increase in toxicity. Ag and Pt form an electrochemical cell and Pt being nobler than Ag in the galvanic series, enhances the release of Ag^+ into the solution. Betts et al. [32] have shown that a higher corrosion current resulted when Ag and Pt is coupled.

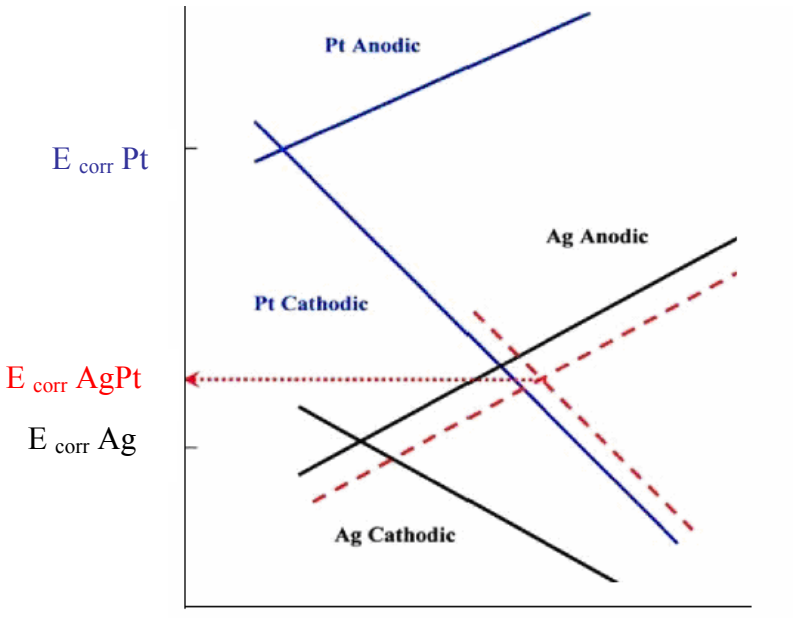

Figure 3.7 Schematic Evans diagram showing location of E_{corr} values for separate and combined silver and platinum metal electrodes [32].

Baker et al. [33] studied the antibacterial effects of silver nanoparticles and found that their activity is dependent on the particle size and showed higher antibacterial activity at smaller sizes. Nanoparticles in the size range of 15 nm have higher surface to volume ratio and hence cover large areas. So even at lower concentration they can provide better antibacterial activity [33, 34, 35].

Dunn and Jones [36] suggested that nanocrystalline silver is a high energy metastable form of elemental silver and when dissolved, releases both Ag^0 and Ag^+. This coat (termed as Acticoat ^{TM}) provides antibacterial effects for longer duration of time and in their case, it was to around 7 days which is substantially better duration of time. Morones et al. [7] have found that almost 95 % of the silver nanoparticles released from the carbon matrix had cuboctahedral and multipled twinned icosahedral and decahedral morphologies and since they all provide {111} surface, they should be highly reactive. They proposed that nanopartclies in the range of 1-10 nm mainly interact with the bacteria and disturb their metabolic activities. So, effective size distribution of the nanoparticle is advantageous for desirable antibacterial properties.

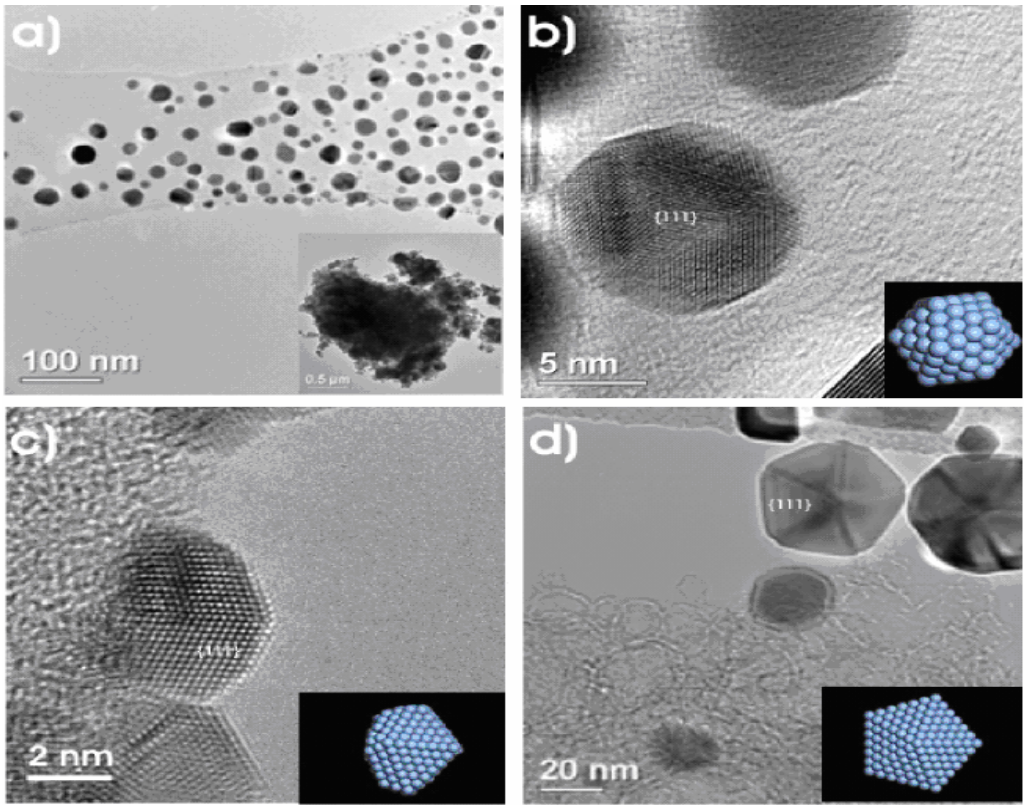

Figure 3.8 Silver nanoparticles. (a) TEM image of the silver nanoparticles that have been released from the carbon matrix; the inset illustrates the agglomerated particles in the carbon matrix. (b)-(d) Most common morphologies of the particles used. The {111} facets are labelled and their respective models are shown as insets: (b) icosahedral particle, (c) twinned particle and (d) decahedral particle seen in the [100] direction [7].

Babonneau et al. [37] deposited Ag in graphite-like carbon by dual ion sputtering and found that at the metal/matrix interface, graphitization of carbon occurs. Initially, metal islands are formed and the spaces between being filled by carbon atoms. The carbon matrix restricts the lateral growth of metallic cluster and the metallic cluster elongates by surface diffusion of the incoming atoms. The carbon matrix, which acts as a diffusion barrier, provides wear resistances and protects the nanoclusters against oxidation.

Although a lot of studies have been done on the efficacy of Ag as an antibacterial agent, there are still issues which need to be explored. Synthesis of Ag-DLC by a hybrid plasma CVD/PVD process has not been attempted yet. This process has been shown to provide DLC and Me-DLC films of high quality. Thus, this route was explored with respect to Ag-DLC.

CHAPTER 4

EXPERMIENTAL DESIGN AND PROCEDURE

A preliminary study of DLC synthesized by using methane and Argon as the precursor gas was conducted using the plasma CVD system to investigate the effect of processing parameters, like DC biasing and working pressure on the film quality and deposition rate. Subsequently, Ag-DLC was synthesized by a hybrid PVD/CVD process. An investigation of the effect of silver content of the DLC on the mechanical, tribological and electrochemical behavior of the films was performed. All the deposition was conducted using the home built hybrid PVD/CVD system. The details of the deposition system are given illustrated below.

4.1 Synthesis of DLC and Ag-DLC film

4.1.1 Hybrid plasma CVD and PVD system.

DLC films were deposited using our home built vacuum system combining Magnetron sputtering and CVD. Figure 4.1 presents a schematic of the system. The stainless steel chamber has a cylindrical shaped with 18.38“ diameter and 19.66” in length. This system has two Magnetron guns (2” diameter) equipped with both, dc and rf biasing capabilities. The guns can hold targets of thicknesses 0.125”, 0.185” and 0.250”. The targets are shielded using a pneumatic shutter over the magnetron gun. The gun is dc biased up to 1kW MDX 1K from Advanced Energy and rf biasing is provided by Seren rf generator and manual matching network. The substrate has rotation, both rf

and dc biasing and heating to 850° C capabilities. The substrate holder has a 4"endplate where the samples to a maximum 4" diameter can be attached. The substrate is dc biased using MDX 10 K from Advanced Energy. Roughing is accomplished down to 25 mtorr by a Trivac 30A mechanical pump and beyond that vacuum is achieved by an Ebara FS 8 series cryopump and compressor. Prior to deposition, the cryopump is roughed down to 25-20 mtorr for 30 mins using the mechanical pump. This helps in partial regeneration of the cryopumps and as such makes it effective in reaching low temperature. After that, the compressor is started to cool the cryoarrays down to 10 K. This helps in creating very clean vacuum inside the chamber during deposition. During the cryo cooling, the gate valve is closed to isolate it from the chamber.

During deposition, very precise pressure control is maintained using an automatic 8"gate valve (Kurt J. Lesker) in conjunction with a MKS 146C PID controller. Three different pressure gages have been installed in the system for different purposes. The thermocouple gage measures the roughing line pressure whereas the baratron measures the chamber pressure during deposition and gives input to the gate valve for maintaining set point pressure. The ion gage measures the pressure when the chamber is exposed to the cryo pump for creating high vacuum. It operates only under a pressure below 10^{-4} mtorr. The gases during deposition are controlled using Unit Instruments mass flow controllers and a read out box.

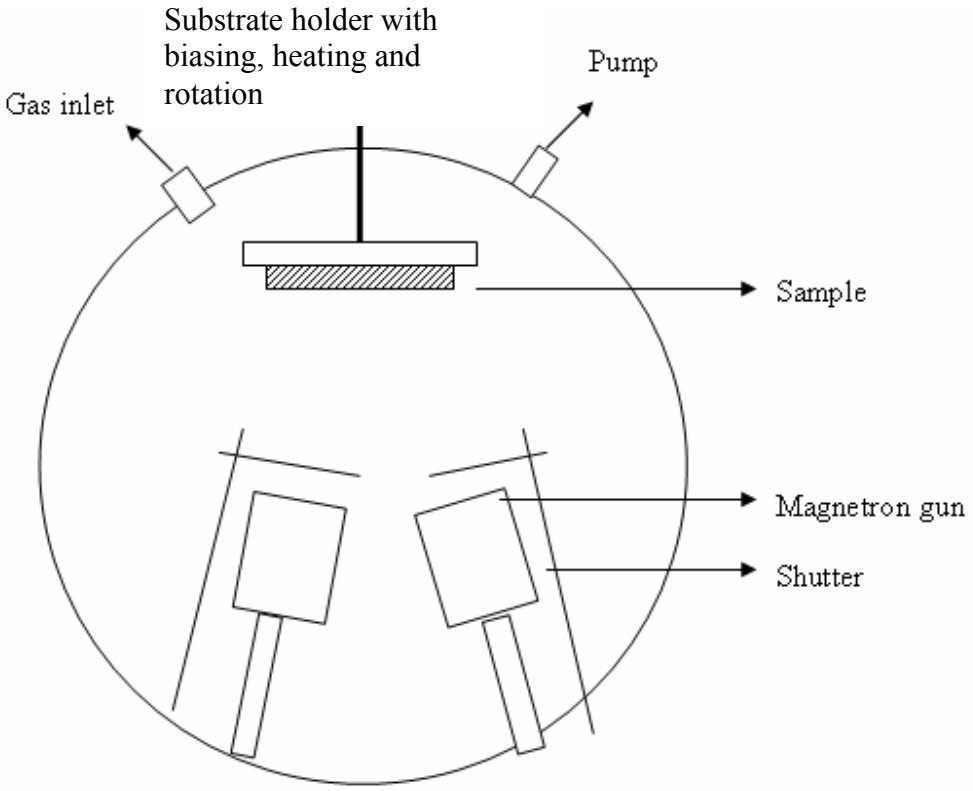

Figure 4.1 Schematic representation of the home built hybrid plasma CVD and PVD system.

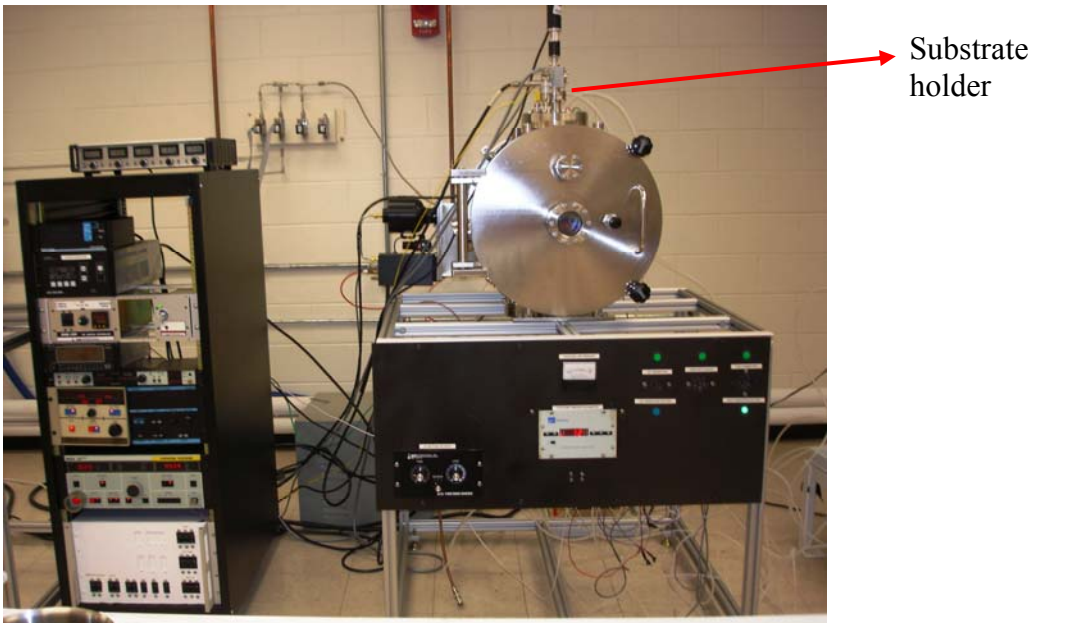

(a)

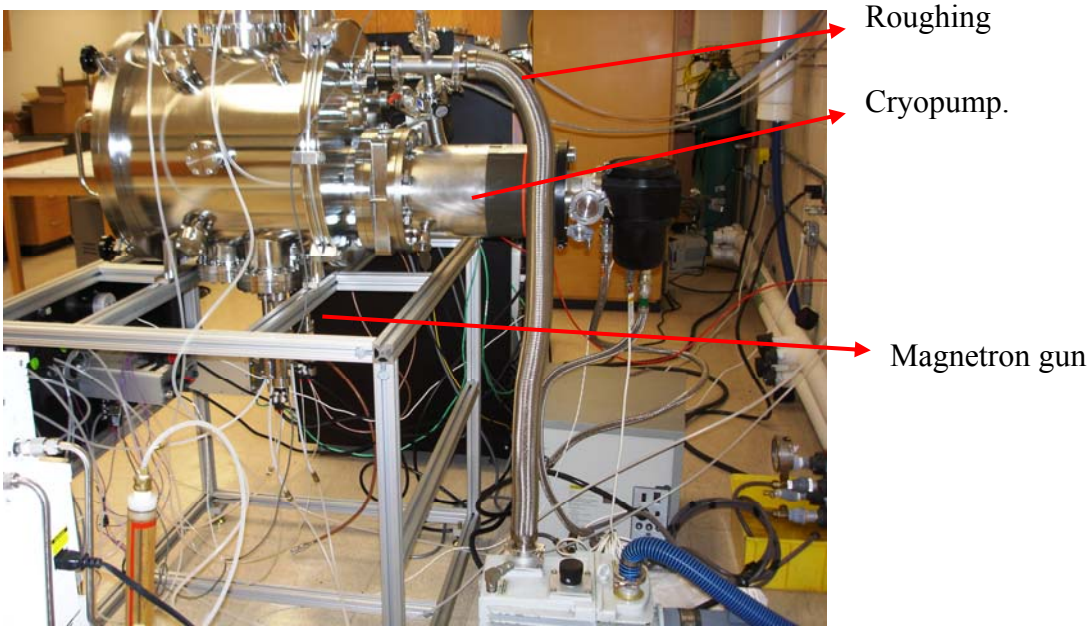

(b)

Figure 4.2 Hybrid plasma CVD and PVD system (a) Front view of the system, (b) Side view of the system.

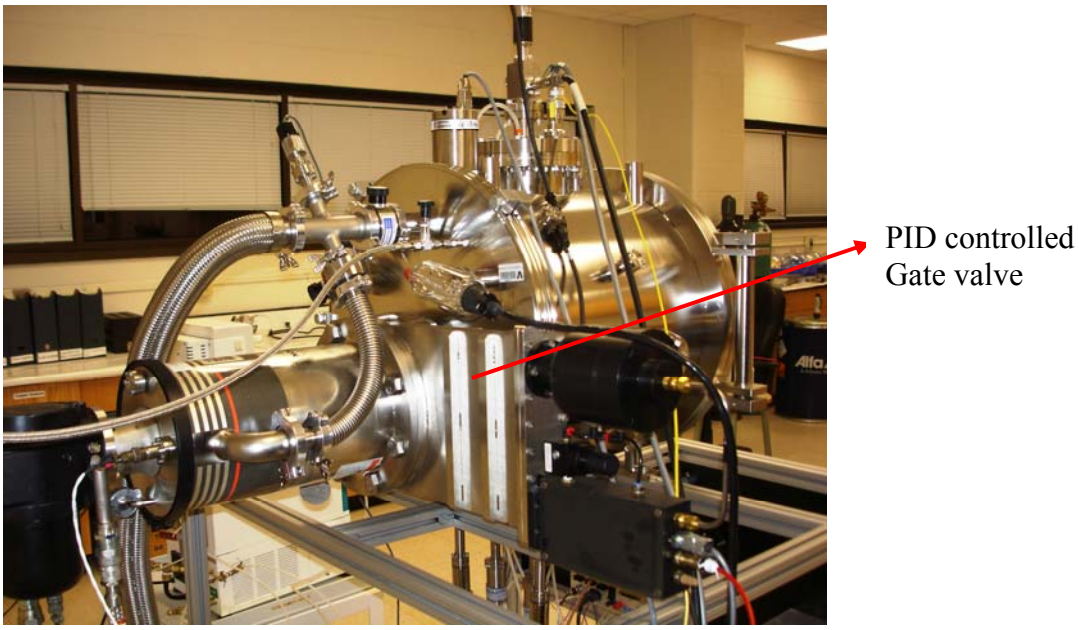

Figure 4.3 Side view of the hybrid plasma CVD and PVD system.

4.2 Procedure for DLC and Ag-DLC deposition

4.2.1 DLC deposition parameters

All DLC and Ag-DLC films were deposited on 2" Si (100) p-type wafers. Prior to deposition, the wafers were cleaned in acetone and then cleaned with compressed air. The wafer was masked in three regions at the edges. These masked regions were later used for measuring the film thickness using step height analysis. The chamber was roughed down to 30 mtorr using the mechanical pump and then the chamber was exposed to the cryopump by opening the gate valve. The base pressure of the chamber was around $1x10^{-6}$ mtorr. The chamber was purged five times with Argon prior to any processing. The substrate was sputtered cleaned with Argon at bias of -1000 V for 15 min at a pressure of 50 mtorr. Sputter cleaning is removing any surface contamination and contributes to good adhesion of the films.

DLC films were deposited by negative biasing of the substrate in a discharge composed of methane and argon atmosphere. The processing parameters are given in the Table 4.1

Table 4.1 DLC deposition parameters.

Sample No	**DC Bias V**	**Pressure (mtorr)**	**CH4/Ar Flow (sccm)**	**Time (hr)**
DLC-1	-600	50	20/4	1
DLC-2	-600	100	20/4	1
DLC-3	-600	100	20/4	1
DLC-4	-600	100	20/4	2.5
DLC-5	-1000	100	20/4	1
DLC-6	-1000	100	20/4	2.5

4.2.2 Ag-DLC deposition parameters

Ag-DLC films were deposited by sputtering Ag with a CH_4/Ar mixture while a negative bias was applied to the substrate. Ag was initially pre-sputtered on the shutter plate to establish good plasma and the shutter was opened when proper plasma was established. The sputtering was conducted in current control mode. The current was varied from 20 mA to 100 mA to vary the Ag content in the DLC films. The working pressure, CH_4/Ar ratio and magnetron current were varied to obtain a wide variety of Ag containing films. The results showed that proper pressure and CH_4/Ar ratio was one

of the key parameters to obtain good quality Ag-DLC films. The deposition parameters are given in the Table 4.2.

Table 4.2 Deposition parameters for Ag-DLC films.

Sample	Bias voltage V	Working Pressure in mtorr	CH_4/ Ar ratio	Total flow sccm	Current in mA	Deposition time hr
Ag-DLC-1	-1000	75	1/2.33	125	20	1
Ag-DLC-2	-1000	75	1/2.33	125	50	1
Ag-DLC-3	-1000	75	1/2.33	125	100	1
Ag-DLC-4	-1000	50	1/3.33	125	20	1
Ag-DLC-5	-1000	50	1/1.33	125	20	1
Ag-DLC-6	-1000	50	1/2.33	125	20	1
*Ag-DLC-7	-1000	50	1/2.33	125	35	3.5
*Ag-DLC-8	-1000	50	1/2.33	125	100	3.5
Ag-DLC-9	-1000	40	1/2.33	125	10	1
Ag-DLC-10	-1000	40	1/2.33	125	20	1
Ag-DLC-11	-1000	40	1/2.33	125	30	1
Ag-DLC-12	-1000	40	1/2.33	125	40	1
Ag-DLC-13	-1000	40	1/2.33	125	50	1
*Ag-DLC-14	-1000	40	1/2.33	125	100	4
*Ag-DLC-15	-1000	40	1/2.33	125	50	4

* Films that were further considered for characterization and analysis

4.3 Characterization of DLC and Ag-DLC films

4.3.1 Thickness and deposition rate

The masked areas of the Si wafers were used to measure the film thickness. The thickness was measured using a stylus profilometer. The profilometer uses a stylus as the sources and it traverses on the masked area and measures the height difference. Figure 4.4 shows the arrangement of the Si wafer and its attachment on the substrate.

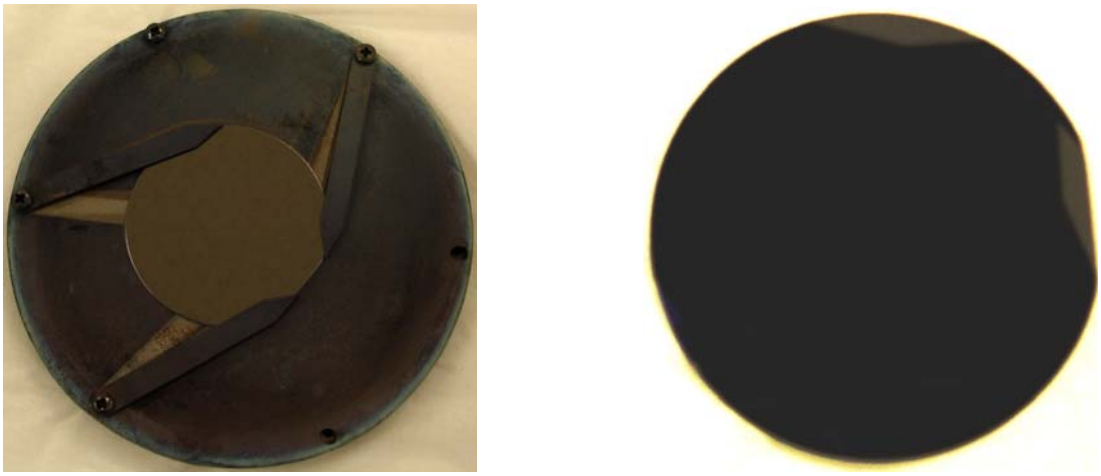

(a) (b)

Figure 4.4 (a) Silicon wafer mounted on the end plate prior to deposition (b) Silicon wafer after deposition with masked areas at the edges.

4.3.2 Microstructural characterization of DLC and Ag-DLC films

4.3.2.1 Scanning Electron Microscopy (SEM)

Scanning Electron Microscopy in conjunction with Energy Dispersive Spectroscopy (EDS) System was used to investigate the cross section morphology of the DLC films and obtain the compositional analysis of the Ag-DLC films.

4.3.2.2 Transmission Electron Microscopy (TEM).

TEM analysis of selected Ag-DLC films was performed using a JEOL JEM 1200 TEM at an accelerating voltage of 120 keV. Thin electron transparent Ag-DLC films were directly deposited on carbon coated copper grids. Based on the previously determined deposition rate, these films were deposited for 20 minutes in order to obtain a thickness of about 20 nm. Examinations were conducted to determine the size and distribution of Ag nanoparticles in the DLC matrix. The structural characterization was conducted by selected area electron diffraction pattern analysis.

4.3.2.3 X-Ray Photoelectron Spectroscopy

XPS was used to investigate the binding energy of C atoms in the DLC and Ag-DLC films. X-rays are irradiated on the sample and the kinetic energy of photo-excited core electrons is determined as a measure of their binding energy. This method is useful for analysis up to a depth of 10nm. XPS spectra were obtained by using a Perkin Elmer digital 500 instrument. The source was Al excited to 300 watts, the spot size was 2x 3mm and the pass energy was 8.95 eV.

The samples were cut into 6 x 6 mm and were mounted onto the holder. The chamber pressure was $2x10^{-9}$ torr. High resolution spectra of the peaks were taken to investigate the chemical state of the carbon atoms. The peaks were deconvoluted using the CASA software. The percentage of sp^2 and sp^3 hybridized state was determined based on their areas.

4.3.2.4 Fourier Transform Infrared Spectroscopy (FTIR).

FTIR was used to characterize the bonding in hydrogenated DLC films. The C-H stretching mode is revealed at 2800-3300 cm^{-1} of the FTIR absorption spectrum. The CH_3 asymmetric stretching vibration occurs at around 2975-2950 cm^{-1} whereas for CH_2, the absorption occurs at about 2930 cm^{-1}. The CH_3 symmetric vibration occurs at about 2865-2885 cm^{-1} and the CH_2 absorption occurs at about 2870-2840 cm^{-1} [14,15]. A Nicolet FTIR system was used for the analysis. The spectrum of DLC and Ag-DLC films was subtracted from the Si wafer background to obtain the absorbance response of the films. The resultant curve was smoothed twice using 25 point smoothing in the OM NIC software. The region for C-H stretching was selected and was subjected to a base line correction. The corrected curve was subjected to Fourier Self Deconvolution to get the component peaks. The deconvoluted peaks were curve fitted in a Gaussian distribution and the area under the component peaks was noted for their percentage determination. Although a direct quantitative analysis of the XPS and FTIR results for quantification of H-content is not possible, an approximate percentage of the H-content can be analyzed.

4.3.3 Mechanical Properties

Hardness is one of the most important properties for DLC films. DLC films are mainly known for high hardness and low wear rates. Microhardness measurements were performed on the DLC and Ag-DLC films using a Knoop indentor (KHN) on Leco LM300AT instrument. Before taking the measurements, the instrument was calibrated for a standard sample and the error was within ± 2 %. The Knoop indentor produces a diamond shaped indentation having approximate ratio between long and short diagonals of 7:1. The depth of indentation is about 1/30 of its length. Hardness is calculated by measuring the longest diagonal of the indentation and this is used in the formula with the load used to calculate KHN

KHN: P/ CL^2

Where P: Load in kg_f

L: Length of the longest diagonal in mm.

C ~ 0.07028, constant of indenter relating projected area of the indentation to the square of the length of the long diagonal.

Five readings were obtained from each film at a load of 25 g_f.

4.3.4 Electrical conductivity.

Sheet resistance measurements were performed on the DLC and Ag-DLC films to determine the change in conductivity of the films as a function of Ag content. Sheet resistance was conducted using a FPP-5000 four point probe. The probing mechanism features a constant force probe head which is rigidly fixed in the housing. The microprocessor based electronics permits direct computation of V/I, sheet or slice

resistivity, and metallization thickness. Unlike most four point probe and probing stations, which move the probe head into the wafer, the FPP-5000 is designed so that the wafer is moved into the probe head.

4.3.5 Tribological characterization of DLC and Ag-DLC films

The tribological behavior of the DLC and Ag-DLC films was investigated by conducting pin-on-disc experiments using a tribometer (CSM instruments). A 440C steel ball of 9.5mm diameter was used as the pin material for the experiments. A load of 5N was applied for the experiments. The wear tests were performed with a linear velocity of 10 cm/s and it was run for a distance of 700m. The friction coefficient was continuously monitored as a function of sliding distance.

The wear rate calculated by observing the wear track profile under an stylus profilometer. The wear volume was measured by multiplying the cross sectional area of the wear track by the length of the wear track. The wear rate of the film is given by

Wear rate = Wear volume (mm^3)/{load (N) x sliding distance (m)}

SEM observations were conducted on the wear tracks and on the pin scar to determine possible transfer layer formation.

4.3.6 Electrochemical behavior of Ag-DLC films

The electrochemical behavior of the Ag-DLC films was investigated by performing anodic polarization testing in deaerated physiological solution. The experiments were performed using an EG&G potentiostat/galvanostat (Model 273 by Princeton Applied Research). The electrolyte used was Phosphate buffer solution (PBS). The PBS solution was prepared by mixing 8 g of NaCl, 0.2 g KCL, 1.44 g

Na_2HPO_4, 0.24 KH_2PO_4 in one liter of distilled water. The pH of the solution was 7.38 which is similar to blood (pH = 7.4). A Standard Calomel Electrode (SCE) was used as the reference electrode and graphite was used as the counter electrode. The electrolyte was deaerated for about 30 minutes by purging Ar prior to initiating the experiment. During the experiment, the potential was swept from -1V below the open circuit corrosion potential E_{corr} to 1V above the E_{corr} and the corresponding current was measured. The potential scanning rate was 5 mV/s. A plot of potential E (mV) vs current density was obtained to evaluate the corrosion behavior. Corrosion rates were determined by Tafel extrapolation to analyze the Ag-DLC films.

CHAPTER 5

RESULTS AND DISCUSSION

5.1 Effect of processing parameters on DLC and Ag-DLC films

5.1.1 DLC films

DLC films were deposited by varying the bias voltage and pressure in accordance with the parameters reported earlier by Gupta et al. [14]. It was observed that better quality DLC films and deposition rate is obtained at a biasing voltage of -1000 V and 100 mtorr pressure. The film quality obtained with these conditions was very good. Very low deposition rate was obtained at biasing voltage of -600 V and 50 mtorr. Prior to all deposition, Argon cleaning was done for 10 minutes at a substrate biasing of -1000V. Initially films were deposited for 1 hour to decide the deposition rate and finally DLC-3 and DLC-5 was deposited for 2.5 hr for hardness measurement and pin-on-disc experiments. DLC-2 was tested to see if HF cleaning of the Si wafer to remove SiO_2 has any effect on the deposition rate. No considerable difference was observed in the deposition rate. Table 5.1 presents the processing conditions and deposition rate of all DLC films from this initial study.

Table 5.1 Deposition rate for DLC films.

Sample name	DC Bias V	Pressure mtorr	CH4/Ar Flow sccm	Time (hr)	HF Cleaning	Thickness (nm)	Deposition Rate (nm/min)
DLC-1	-600	50	20/4	1	No	14.1	0.23
DLC-2	-600	100	20/4	1	Yes	112.37	1.87
DLC-3	-600	100	20/4	1	No	104.72	1.74
DLC-4	-600	100	20/4	2.5	No	223.7	1.49
DLC-5	-1000	100	20/4	1	No	349.625	5.82
DLC-6	-1000	100	20/4	2.5	No	940.25	6.26

5.1.2 Ag-DLC films

During Ag-DLC deposition, it was observed that the working pressure is very critical for controlling the Ag content in DLC. A series of experiments were performed to obtain a varying Ag content in DLC. At high pressure, it was observed that formation of DLC is predominant even at high magnetron currents. The films were non uniform in Ag content. An optimum pressure for Ag-DLC was selected in the range 40-50 mtorr and variation in Ag content was achieved by varying the magnetron current. In addition to pressure, the CH_4/Ar ratio plays a very important role in Ag-DLC deposition. An improper ratio results in carbon on the target. A high ratio results in high Ag sputtering and minimum DLC was formed. The film was uniform but non adherent. An optimum ratio of 1:2.33 was selected from the analysis from a series of depositions. This ratio resulted in uniform and good quality films. Four films namely Ag-DLC-7, Ag-DLC-8,

Ag-DLC-14 and Ag-DLC-15 having silver content 2.5 at.%, 5 at.%, 34 at.% and 21.3 at.% were selected for analysis.

Table 5.2 Composition analysis of Ag-DLC films.

Sample	**Thickness nm**	**EDS analysis**	
		at.% C	**at.% Ag**
Ag-DLC-1	32	95.5	4.5
Ag-DLC-2	45	97	3
Ag-DLC-3	32	97.1	2.9
Ag-DLC-4	48	28	72
Ag-DLC-5	42	97	3
Ag-DLC-6	36	94	6
*Ag-DLC-7	425	97.5	2.5
*Ag-DLC-8	367	95	5
Ag-DLC-9	29	96.25	3.75
Ag-DLC-10	23.5	95.4	4.6
Ag-DLC-11	27	93.28	6.72
Ag-DLC-12	31	91.98	8.02
Ag-DLC-13	113	79.18	20.82
*Ag-DLC-14	477	66	34
*Ag-DLC-15	510	78.7	21.3

*These films were selected for characterization

5.2 Characterization of DLC and Ag-DLC films

5.2.1 Film microstructure

5.2.1.1 Scanning Electron Microscopy

Fractured cross sections of the DLC-6 and Ag-DLC-7 films were observed under SEM to investigate the adhesion of the film to the surface. Figure 5.1 and 5.2 shows the interface between Si wafer and the films. It showed featureless films without porosity or other visible defects. There was no visible separation or gaps between the substrate and the film indicating that the films have good adhesion to the substrate.

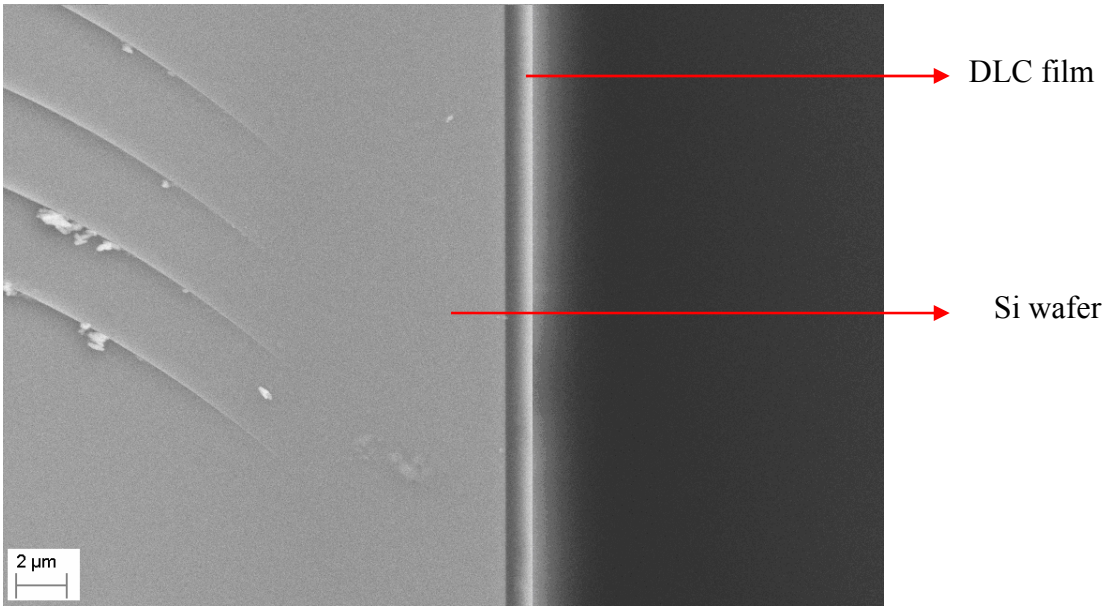

Figure 5.1 SEM micrograph showing cross section of DLC-6 film.

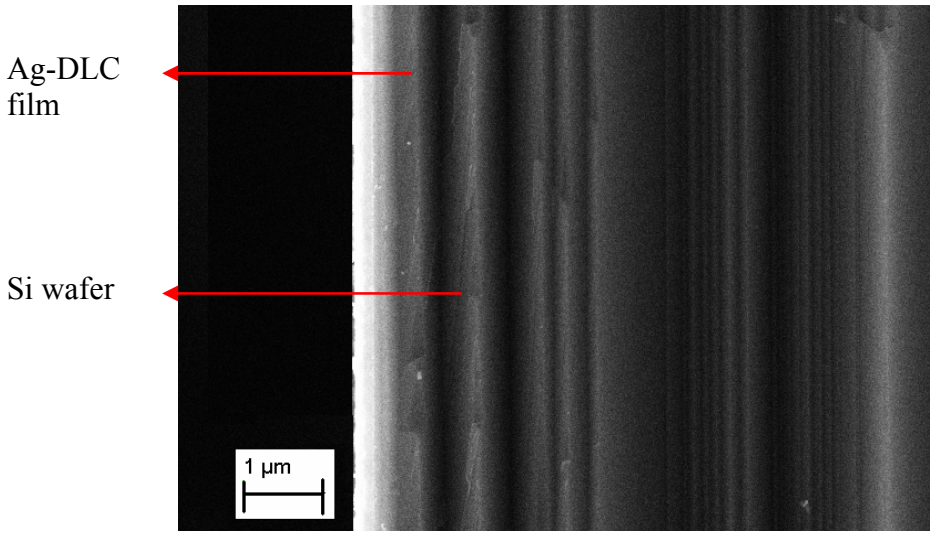

Figure 5.2 SEM micrograph showing cross section of Ag-DLC-7 film.

5.2.1.2 Transmission Electron Microscopy

Ag-DLC films were deposited directly on copper grids using the same parameters of Ag-DLC-13 film for 20 minutes. The plan view TEM image is shown in Figure 5.3 Ag nanoparticles are found to be uniformly distributed in the DLC matrix. The nanoparticle size ranges from 5-8 nm and they are separated from each other by around 2-3 nm of DLC. The SAED pattern reveals two difussed rings indicating diamond like carbon structure followed by two sharp rings indicating the presence of Ag. The d-spacing of the rings was indexed and it corresponds to Ag (111) and (200).

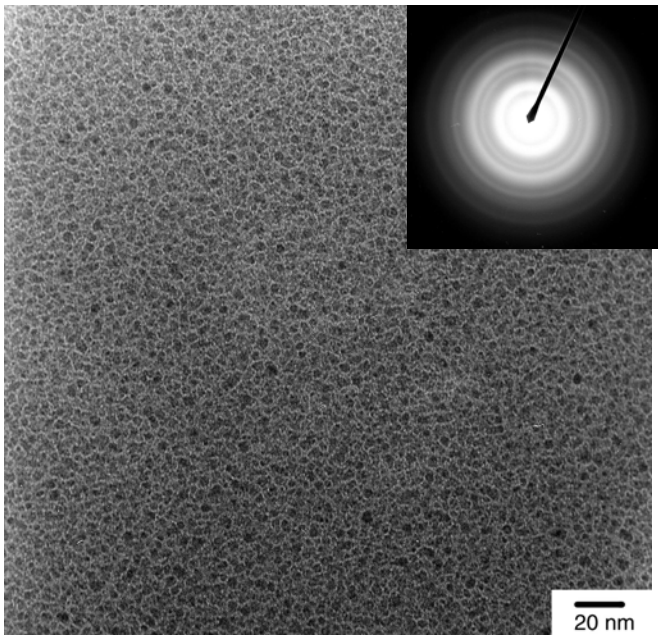

Figure 5.3 Plan view TEM image of Ag-DLC film.

5.2.1.3 X-ray Photoelectron Spectroscopy

Three films namely, DLC-6, Ag-DLC-8 and Ag-DLC-14 were investigated using XPS to determine their sp^2 and sp^3 content. XPS yields important results which are helpful in optimization of the DLC synthesis process. Figure 5.4 and 5.5 shows the high resolution XPS spectra of C 1s peak binding energy. The peak was deconvoluted into two components with binding energy of 284.3 eV and 284.8 eV corresponding respectively, to sp^2 and sp^3 C-C and C-H bonding in the film. In the Ag-DLC, a third component was obtained revealing Ag-C bonding.

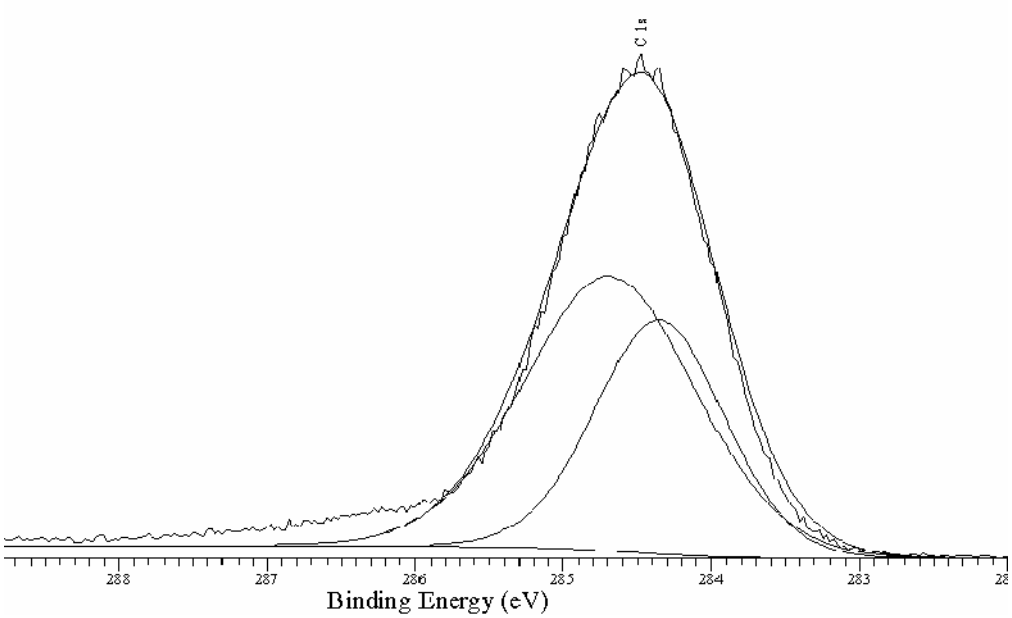

(a)

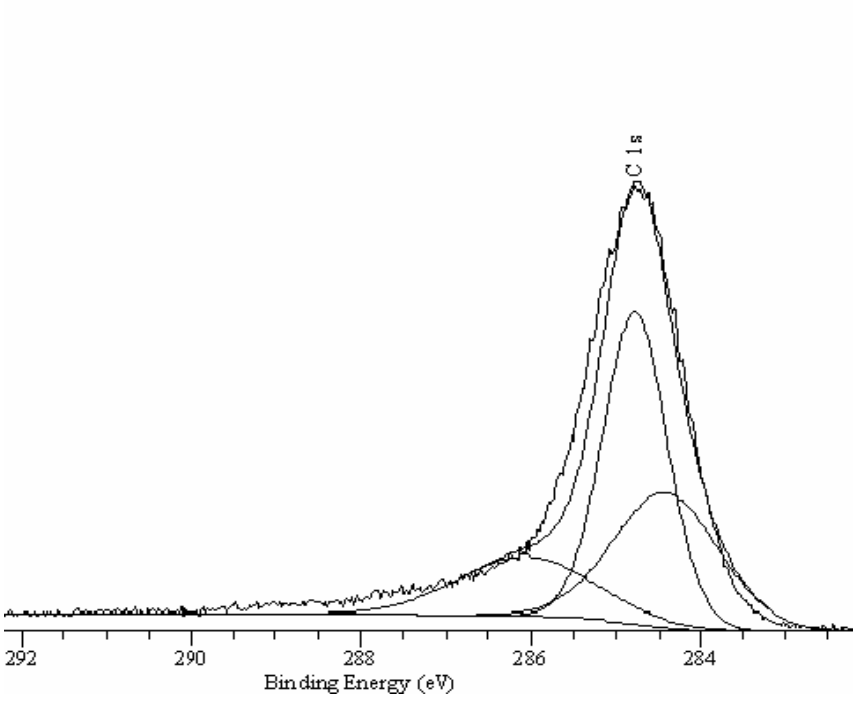

(b)

Figure 5.4 High-resolution C1s XPS spectrum of (a) DLC-6 film (b) Ag-DLC-8 (5 at.% Ag) film

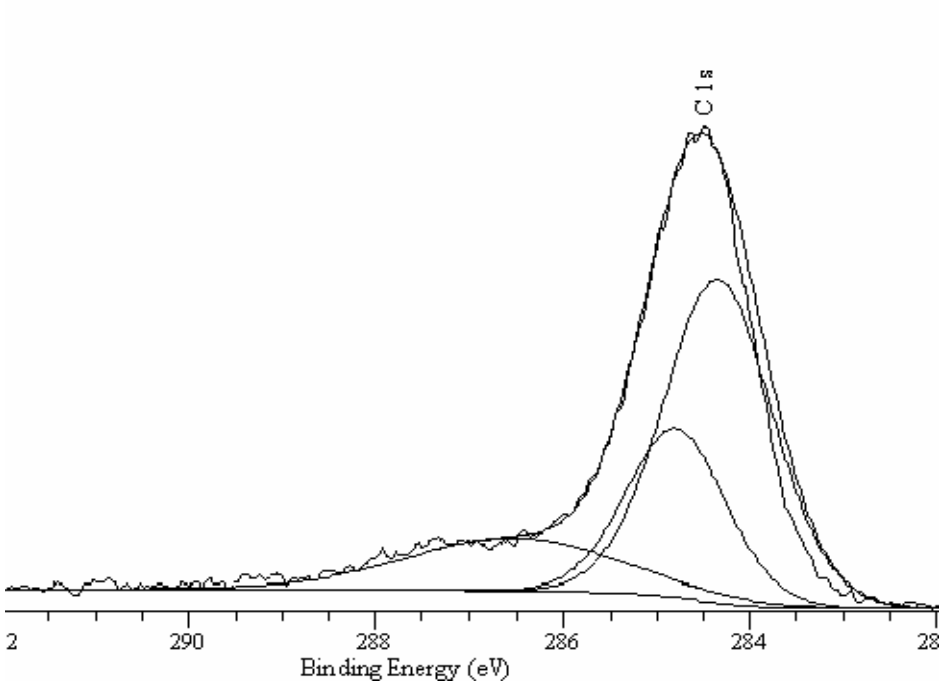

Figure 5.5 High-resolution C1s XPS spectrum of Ag-DLC-14 (34 at.% Ag) film.

Table 5.3 XPS spectra analysis for DLC and Ag-DLC film

Film	Binding energy (eV)			% sp^2	% sp^3	% Ag-C
	sp^2	sp^3	Ag-C			
DLC-6	284.3	284.8	--	33.16	66.84	---
Ag-DLC-8	284.3	284.8	286.4	30.14	51.92	17.32
Ag-DLC-14	284.3	284.8	286.5	55.58	26.66	17.74

The XPS spectra show that as the Ag content increases, the sp^3 content decreases. Similar trends have been observed for other metal doped DLC films [13, 17]. This is in confirmation with the hardness results which reveal similar trends. As the sp^3 content decreases, the films hardness also decreases.

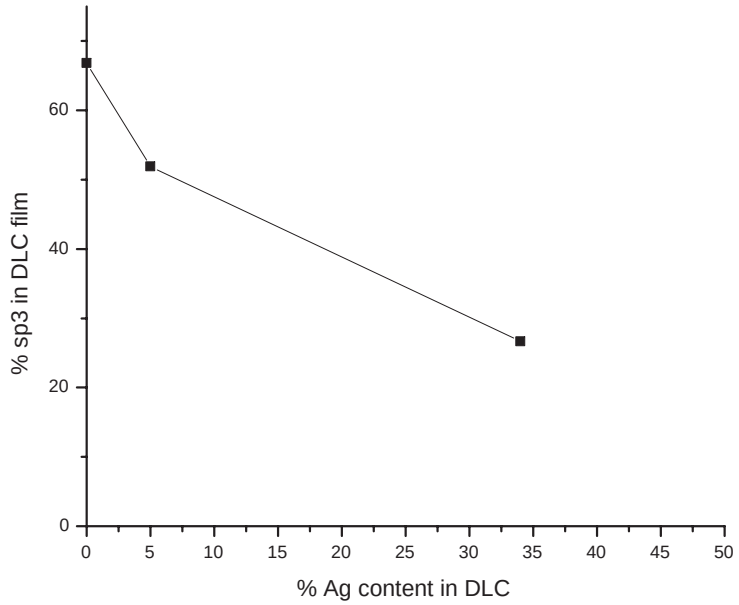

Figure 5.6 Variation of sp^3 C-C bonding with increasing Ag content.

5.2.1.4 Fourier Transform Infrared Spectroscopy

FTIR spectra were taken for DLC-6 and Ag-DLC-7 films to investigate the C-H bonding in the films. Strong FTIR absorption of the C-H stretch was obtained in the range 2800 cm^{-1} and 3100 cm^{-1} which reveals a high H content in the films. Tables 5.4 and 5.5 show the various bonding states of the C-H stretching and also the role of Ag in the DLC film. The relative amount of each bonding type was obtained by estimating the area under each peak. The DLC-6 film has around 80 % sp^3 C-H bonding whereas films Ag-DLC-7 (2.5 at.% Ag) has around 68 % sp^3 C-H bonding. This result shows that both the films have high C-H sp^3 content which is in agreement with the XPS results. XPS results show the sp^3 content from C-C and C-H bonding whereas FTIR refers to the C-H bonding. Although a direct quantification of the H-content is not

possible from the FTIR and XPS results, a general idea can be drawn about the C-C and C-H bonding state.

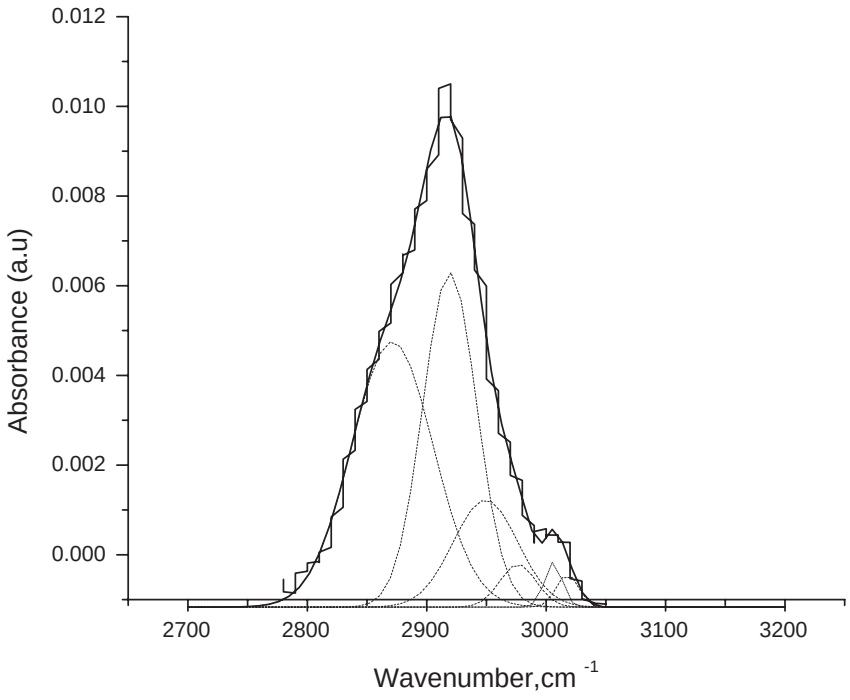

Figure 5.7 Deconvolution of the C-H stretch for DLC-6 film.

Table 5.4 FTIR vibrational mode assignment in the C-H stretch region for DLC-6 film.

Wavenumber, cm^{-1}	**Assignment**	**Peak contribution, %**
2871.3	sp^3 C-H,C-H_2,C-H_3	43.6
2919.3	sp^3 C-H_2,C-H	36.23
2949.3	sp^2(olef) C-H_2	13.93
2976.4	sp^3 C-H_3	3.1
3006.1	sp^2 (olef)C-H	1.4
3017.6	sp^2 (olef)C-H_2	1.5

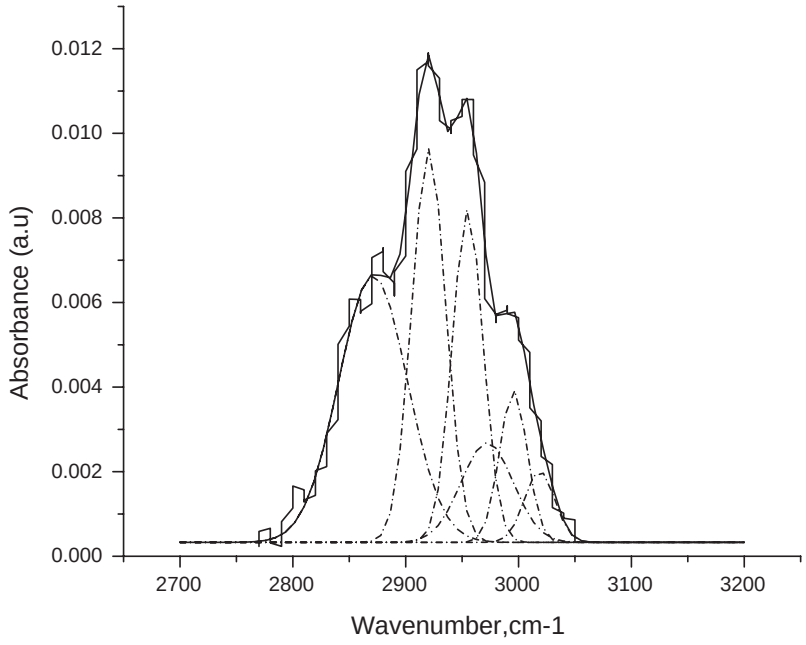

Figure 5.8 Deconvolution of the C-H stretch for Ag-DLC-7 (2.5 at.% Ag) film

Table 5.5 FTIR vibrational mode assignment in the C-H stretch region for Ag-DLC-7 (2.5 at.% Ag) film.

Wavenumber, cm^{-1}	**Assignment**	**Peak contribution, %**
2871.1	sp^3 C-H,C-H_2,C-H_3	34.31
2920.5	sp^3 C-H_2,C-H	24.92
2955	sp^2(olef) C-H_2	19.18
2972.2	sp^3 C-H_3	9.6
2995.5	sp^2 (olef)C-H	7.8
3018.6	sp^2 (olef)C-H_2	4.1

5.2.2 Tribological testing and mechanical properties of DLC and Ag-DLC thin films

Pin-on-disc experiments were performed on samples DLC-6, Ag-DLC-7 and Ag-DLC-8 films. It was observed that the friction coefficient decreases with time as shown in Figure 5.9. This is mainly due to wear induced graphitization occurring at the contact point and is in accordance with the model proposed by Liu and Meletis [19]. Since the thickness of Ag-DLC films was thinner, the test was run for 1000 m for DLC and 700 m for Ag-DLC-7 and Ag-DLC-8 respectively. The wear tracks obtained after the experiment were measured by stylus profilometer for wear rate measurement.

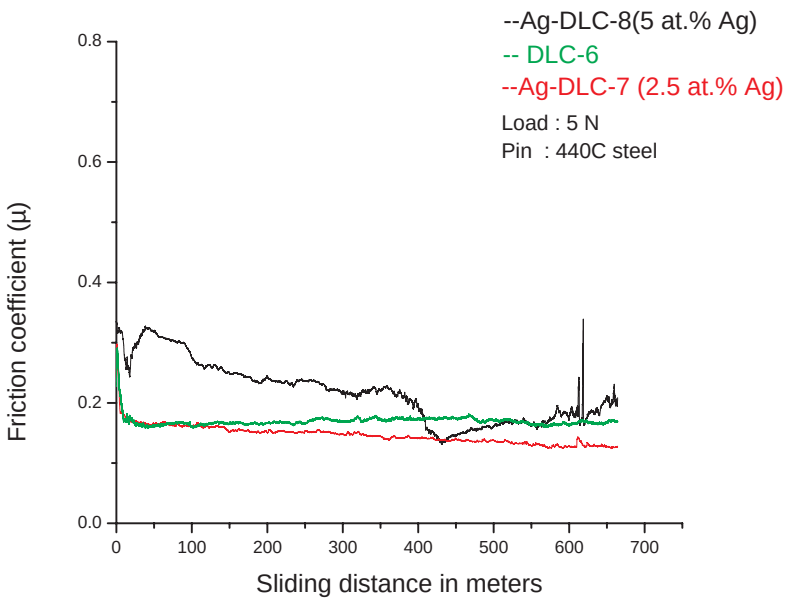

Figure 5.9 Coefficient of friction of DLC and Ag-DLC films.

Microhardness results of the DLC and Ag-DLC films are shown in the Figure 5.10. It is seen that with increase in Ag content in DLC films, the hardness value decreases. With increase in metal content, the sp3 content decreases resulting in lower hardness. This trend has been observed in other Me-DLC [13,17]. Singh et al. [38] investigated the mechanical properties of Cr-DLC and reported that DLC hardness is also from the compressive residual stresses in DLC. In Me-DLC, the C-C network is broken down by the presence of Me nanoparticles and this results in decrease in hardness. Also, it has been observed that most C in the Me/matrix interface is sp^2 interface.

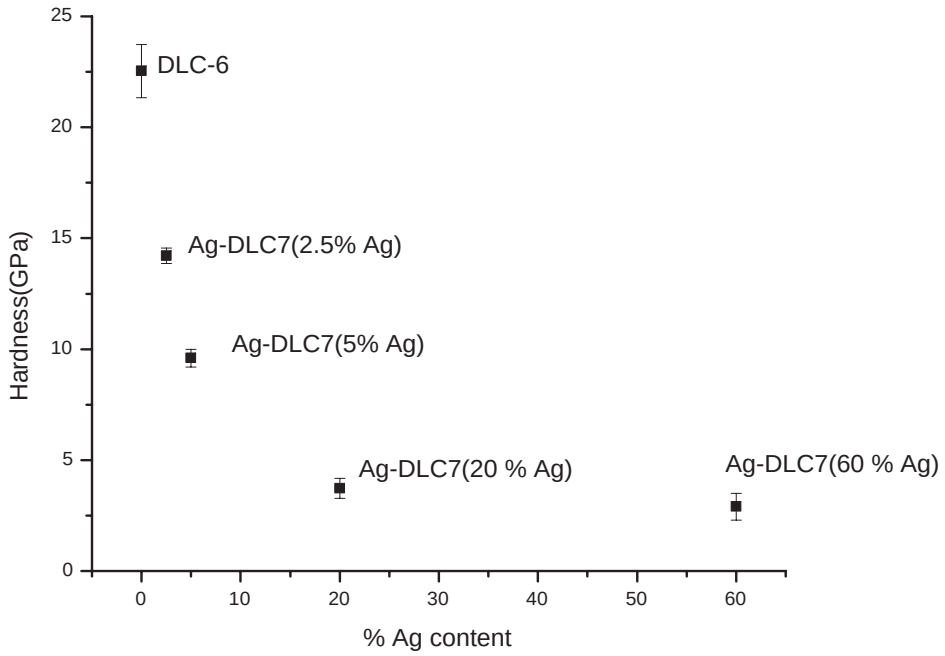

Figure 5.10 Koop Hardness value of DLC and Ag-DLC as a function of silver content of DLC films.

5.2.2.1 Wear behavior

The morphology of the wear tracks of DLC-6 and Ag-DLC-7 and Ag-DLC-8 were measured by stylus profilometer and the wear rates were calculated. The DLC-6 wear track shows wide track with low depth suggesting a short range material removal. This is due to hard DLC film showing minimum wear. Ag-DLC-7 (2.5 at.% Ag) and Ag-DLC-8 (5 at.% Ag) has higher depth wear track, suggesting more removal with the increase in Ag doping. Table 5.6 shows the variation of wear rate with Ag doping.

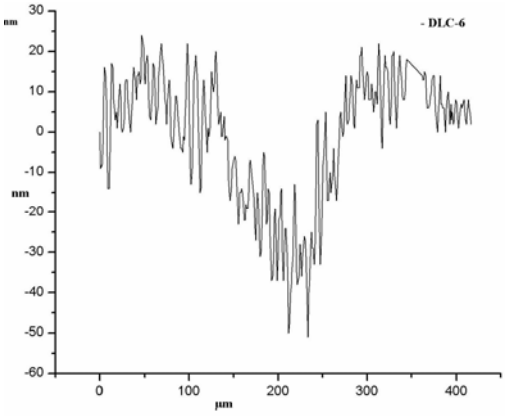

(a)

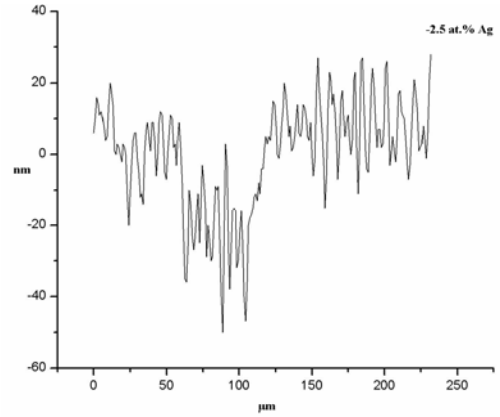

(b)

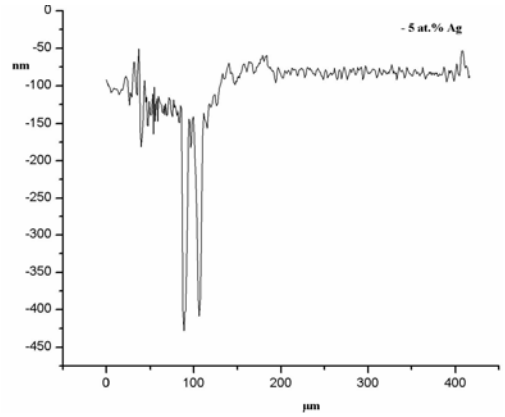

(c)

Figure 5.11 Wear track morphology of (a) DLC-6 (b) Ag-DLC-7 (2.5 at.% Ag) and (c) Ag-DLC-8 (5 at.% Ag) film

Table 5.6 Wear rate of DLC and Ag-DLC films

Sample	**Wear rate mm^3/Nm**
DLC-6	1.9×10^{-8}
Ag-DLC-7	2×10^{-7}
Ag-DLC-8	8×10^{-7}

5.2.2.2 Transfer layer behavior of DLC and Ag-DLC films

SEM was conducted on the pin after wear testing. EDS analysis of DLC revealed that debris included carbon whereas for Ag-DLC it includes both Ag and carbon. Low friction and low wear rate in DLC is explained by a transfer layer build up in the pin. A significant wear in the initial stages might have created a graphitic transfer layer resulting in decrease in friction coefficient in the long run. Rough transfer layer was observed in Ag-DLC pin ball indicating high wear of the film. This might be due to the presence of Ag nanoparticle in the film which is soft compared to the amorphous DLC matrix. Discontinuity of transfer layer was observed if a significant amount of Ag nanoparticles was present. Singh et al. [38] reported similar observation in Cr-DLC and suggested that beyond a certain level (Cr content > 4.8 at.%), the amount of DLC present is not sufficient to form a continuous layer providing the necessary lubrication and so chromium carbide that wears out faster dominates the wear process.

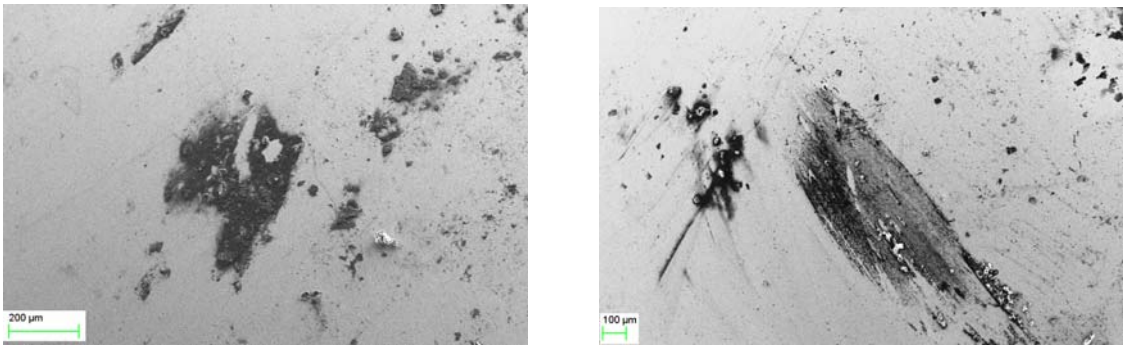

(a) (b)

Figure 5.12 SEM of the pin after wear testing (a) DLC-6 and (b) Ag-DLC-8 (5 at.% Ag) film

5.2.3 Electrical conductivity of Ag-DLC films.

Sheet resistance of DLC-6, Ag-DLC-4, Ag-DLC-14 and Ag-DLC-15 films were measured using a four point probe. The sheet resistance of the bare Si wafer was found to be 3.93 X 10^2 ohms/square. DLC-6 was highly dielectric and showed high resistance value. The sheet resistance decreases with increasing Ag content, making the film more and more conductive.

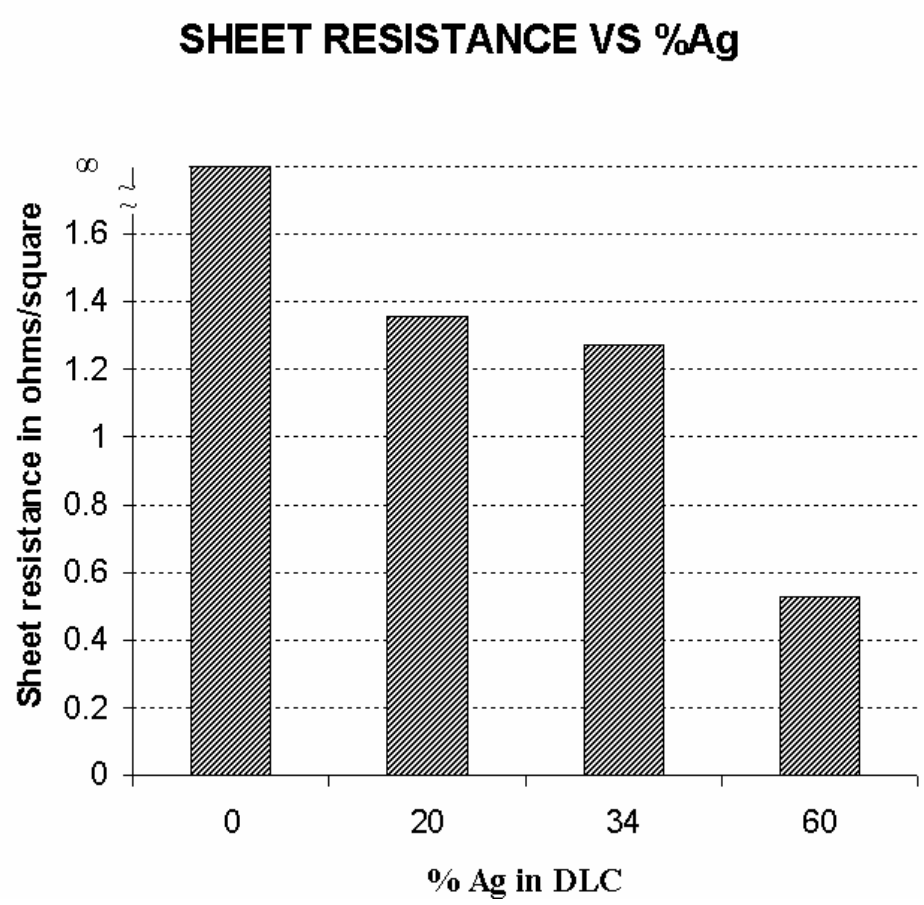

Figure 5.13 Variation in sheet resistance with increasing Ag content in DLC films.

5.2.4 Electrochemical behavior of pure silver and Ag-DLC films

Anodic polarization experiments were performed on Ag-DLC-4, Ag-DLC-8 and pure silver in PBS solution under dearated conditions. An area of 1 cm^2 was selected and the rest of the sample was protected from exposure to the electrolyte. The sample was immersed in the electrolyte and the solution dearated for 30 min before anodic polarization scan was initiated.

The anodic polarization curves show that with increasing silver content the current density increases leading to higher anodic currents. This indicates that more Ag dissolves into the electrolyte. This is in accordance with the lowering corrosion potential of the films with Ag content.

The results show that in Ag-DLC, silver ions are released in the solution during electrochemical experiments. This is an important parameter for the potential application of Ag-DLC in biomedical application. Figure 5.14 and 5.15 present the anodic polarization behavior of the three films tested.

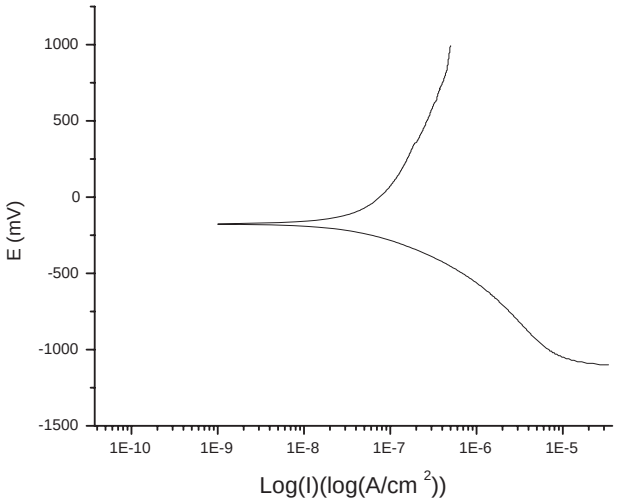

(a)

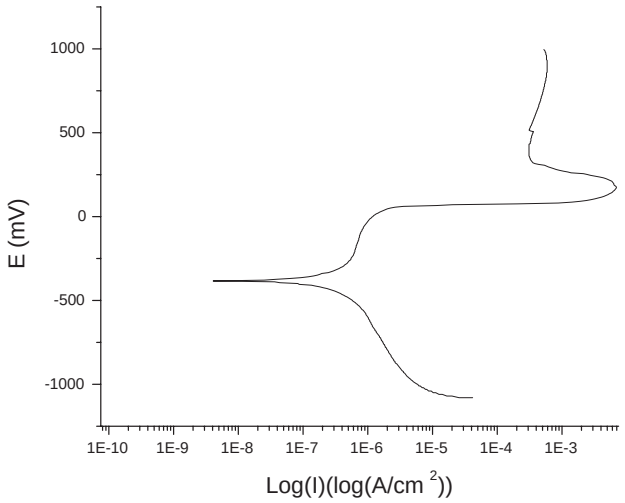

(b)

Figure 5.14 Anodic polarization curves of films (a) Ag-DLC-8 (b) Ag-DLC-4

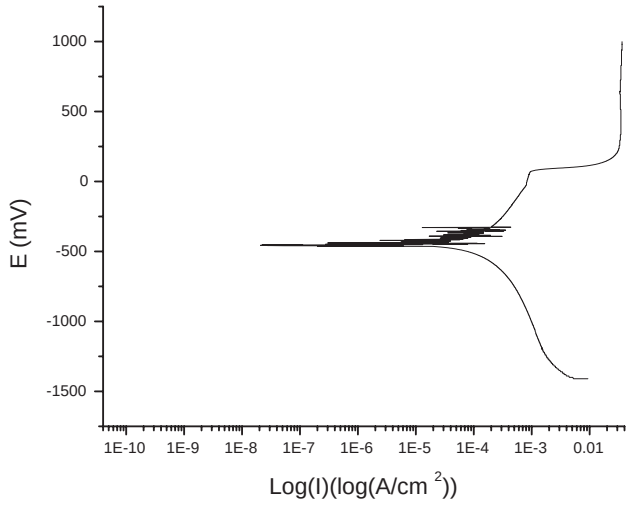

Figure 5.15 Anodic polarization curve of pure silver

Table 5.7 Electrochemical behavior of Ag-DLC films

Sample	**Potential(SCE) mV**	**Current density nA/cm^2**
Ag-DLC-8 (5 at. % Ag)	-174.9	13.84
Ag-DLC-4 (72 at.% Ag)	-383.2	101.4
Pure Ag	-460.4	176.4 X 10^3

CHAPTER 6

CONCLUSIONS

The following conclusions can be drawn from the present study:

1. A preliminary study was conducted and processing conditions were identified to produce quality DLC films.
2. Based on the initial study, Ag-DLC films were synthesized with varying Ag content and characterized in terms of structure, mechanical and tribological and corrosion behavior. An attempt was made to make a comparative study between DLC and Ag-DLC films.
3. TEM observation revealed that the films contain of uniformly distributed Ag nanoparticles of sizes 5-8 nm in an amorphous DLC matrix and the particles were separated by 2-3 nm DLC matrix.
4. The friction coefficient for DLC and low silver content (~5 at.% Ag) were found to be comparable while maintaining a low wear rate.
5. Anodic polarization results reveal that Ag-DLC has lower current density than pure silver, making it more inert than pure silver.
6. The doping of DLC with Ag resulted in decrease in sheet resistance of the Ag-DLC making it more conductive compared to dielectric DLC films.

REFERENCES

1. J. Robertson, Diamond like amorphous carbon, Material science and engineering, R 37, (2002), 129.
2. Q. L. Feng, J. Wu, G. Q. Chen, F. Z. Cui, T Kim, J Kim, A mechanistic study of the antibacterial effect of silver ions on Escherichia coli and Staphylococcus aureus, Journal of Biomedical Material Research, 52, (2000), 662.
3. N. Ali, Y. Kousar, T. L. Okpalugo, V. Singh, M. Pease, A. A. Ogwu, J. Gracio, E. I. Meletis, M. J. Jackson, Human micro-vascular endothelial cell seeding on Cr-DLC thin films for mechanical heart valve applications, Thin Solid Films, 515, (2006), 59.
4. A. Olborska, M. Swider, R. Wolowiec, P. Niedzielski, A. Rylski, S. Mitura, Amorphous carbon – biomaterial for implant coating, Diamond and Related materials, 3, (1994), 899.
5. D. Tobler and L Warner, Nanotech Silver Fights Microbes in Medical Devices, Medical Device & Diagnostic Industry 27, 5, (2005), 164.
6. U. Klueh, V. Wagener, S. Kelly, A. Johnson, J.D. Bryers, Efficacy of silver coated fabric to prevent bacterial colonization and subsequent device-based biofilm formation, Journal of Biomedical Material Reseasrch, 53, (2000), 621.
7. Morones, Elechiguerra, Camacho, Holt, Kouri, Ramirez, Yacaman, The bacterial effect of silver nanoparticles, Nanotechnology, 16, (2005), 2346.

8. R. J. Narayan, H. Wang, A. Tiwari, Nanostructured DLC-Ag composites for biomedical applications, Material Research Society Symposium Proceedings, 750, (2003), 205.
9. J. Vetter, M. Stuber, S. Ulrich, Growth effects in carbon coating deposited by magnetron sputtering. Surface and Coating technology, 168, (2003), 169.
10. N. Savvides, B. Window, Diamond like amorphous carbon films prepared by magnetron sputtering of graphite, Journal of Vacuum Science Technology, 3(6), (1985), 2386.
11. L. R. Shaginyan, A. A. Onoprienko, V. F. Britun, V.P. Smirnov, Influence of different physical factor on microstructure and properties of magnetron sputtered amorphous carbon films, Thin Solid Films, 397, (2001), 288.
12. A. Grill, Plasma Deposited diamond like carbon and related materials, IBM Journal Research and Development, 43, (1999), 147.
13. C. Corbella, M.Vives, A. Pinyol, E. Bertan, C. Canal, M. C. Polo, J. L. Andujar, Preparation of metal(W, Mo, Nb, Ti) containing a-C:H films by reactive magnetron sputtering, Surface and Coating Technology, 1777-1778, (2004), 409.
14. P. Gupta, V. Singh, E. I. Meletis, Tribological behavior of plasma-enhanced CVD a-C:H films. Part I: effect of processing parameters, Tribology International, 37, (2004), 1019.
15. P. Gupta, E. I. Meletis, Tribological behavior of plasma-enhanced CVD a-C:H films. Part II : multilayers, Tribology International, 37, (2004), 1031.

16. J. Robertson, Mechanism of sp^3 bond formation in the growth of diamond like carbon, Diamond and Related Materials, 14, (2005), 942.
17. C. P Klages and R. Memming, Microstructure and Physical properties of Metal-containing hydrogenated carbon films, Material Science Forum, 52-53, (1989), 609.
18. Y. Chang, D. Y. Wang, W. Wu, Catalysis effect of metal doping on wear properties of diamond like carbon films deposited by a cathodic arc activated deposition process, Thin Solid Films, 40-421, (2002), 241.
19. Y. Liu, E. I. Melitis, Evidence of Graphitization of Diamond-like carbon film during sliding wear. Journal of Material Science, 32, (1997), 3491.
20. N. S. Tambe, B.Bhusan, Nanoscale friction-induced phase transformation of diamond like carbon, Scripta Materialia, 52, (2005), 751.
21. R. Hauert, A review of modified DLC Coating for biological applications, Diamond and related Materials, 12, (2003), 583.
22. E. Mitura, S. MItura, A. Jakubowski, J. Szmidt, A. Sokolowska, P. Louda, J. Marciniak, B. Koczy, Diamond like carbon coatings for biomedical applications, Diamond and Related Materials, 3, (1994), 896.
23. G. Dearnaley and J. H.Arps, Biomedical applications of diamond like carbon (DLC) coatings: A review, Surface & Coating Technology, 200, 2005, 2518.
24. C. P. Lungu, Nanostructure influence on DLC-Ag tribological coating, Surface & Coating Technology, 200, (2005), 198.

25. Furno, Kelly, Wong, Sharp, Arnold, Howdle, Bayston, Brown, Winship and Reid, Silver nanoparticles and polymeric medical devices: a new approach to prevention of infection?, Journal of Antimicrobial Chemotherapy (2004), 54,1019 -1024
26. Fruno, Bayston, Encyclopedia of Biomaterials and Biomedical Engineering, 1, (2004), 34.
27. I. Sondi and B. S. Sondi, Silver nanoparticles as antimicrobial agent: a case study on E.coli as a model for gram-negative bacteria, Journal of Colloid and interface Science, 275, (2004), 177.
28. Morrison, Buchanan, Liaw, Berry, Brigmon, Riester, Abernathy, Jin, Narayan, Electrochemical and antimicrobial properties of diamond like carbon-metal composite films, Diamond & related Material, 15, (2006), 138.
29. A. Ewald, S. K. Gluckermann, R. Thull, U. Gbureck, Antibacterial titanium/silver PVD Coatings on titanium, Biomedical Engineering Online,5, (2006), 22.
30. Schierholz, Lucas, Rump, Pulver, Efficacy of silver coated medical devices, Journal of Hospital infection, 40, (1998), 257.
31. Dowling, Betts, Pope, McConnell, Eloy, Arnaud, Anti-bacterial silver coatings exhibiting enhanced activity through the addition of Platinum , Surface and Coating Technology, 163-164, (2003), 637.
32. Betts, Dowling, McConnell, Pope, The influence of platinum on the performance of silver-platinum anti-bacterial coatings, Materials and Design, 26, (2005), 217.

33. C. Baker, A. Pradhan, L. Pakstis, D. J. Pochan, S. I. Shah, Synthesis and antibacterial properties of silver nanoparticles, Journal of Nanoscience and Nanotechnolgy, 5, (2005), 244.

34. D. Lee, R. E. Cohen, M. F. Rubner, Antibacterial Properties of Ag Nanoparticles Multilayer and Formation of Magnetically Directed Antibacterial Microparticles. Langmuir, 21, (2005), 9651.

35. S. Pal, Y. K. Tak and J. M. Song, Does the antibacterial activity of silver nanoparticle depend on the shape of the nanopartcile ? A Study of the Gram-Negative bacterium Escherichia coli, Applied and Environmental Microbiology, 73, (2007), 1712.

36. K. Dunn and V. E.Jones, The role of Acticoat^{TM} with nanocrystalline silver in the management of burns, Burns,30 suppl. 1, (2004), S1.

37. D. Babonneau, J. Toudaert, S. Camelio, F. Pailloux, T. Cabioc'h, T. Girardeau, Encapsulation of metallic nanoclusters in carbon and boron nitride thin films prepared by ion-beam sputtering, Surface & coating Technology, 200, (2006), 6251.

38. V. Singh, J. C. Jiang, E. I. Meletis, Cr-Diamondlike carbon nanocomposie films: Synthesis, characterization and properties, Thin Solid Films, 489, (2005), 150.

BIOGRAPHICAL INFORMATION

Mr. Pankaj Jyoti Hazarika was born in Sonitpur, Assam, India on 14th of August, 1980. He got his primary education from Don Bosco High School, Tezpur and intermediate from Shrimanta Shankar Academy,Guwahati. He earned his Bachelor of Engineering in Metallurgical Engineering from Visvesvaraya National Institute of Technology, Nagpur, India in 2003. He worked in Essar Steel Limited, Surat, India, for two and half years as production engineer. In fall 2005, he joined University of Texas at Arlington in the Material Science and Engineering department to pursue a Master of Science degree. Currently, he is a candidate for the degree of Master of Science in Material Science and Engineering to be awarded in December, 2007.